Wireless Multicarrier Communications

where Fourier Meets Shannon

Zhengdao Wang and Georgios B. Giannakis
{zhengdao,georgios}@ece.umn.edu
Dept. of ECE, University of Minnesota, 200 Union Street SE, Minneapolis MN 55455, USA

Abstract — Relying on basic tools such as eigen-signals of linear time-invariant systems, linear and circular block convolution and Fast Fourier Transforms, this paper develops a systematic discrete-time framework and designs novel systems for single- and multi-user wireless multi-carrier communications — a field rich in signal processing challenges that holds great potential in various applications including audio/video broadcasting, cable television, modem design, multimedia services, mobile local area networks and future generation wideband cellular systems.

This is a personal copy of the IEEE SP Magazine paper of the same title. It is provided because the official copy has low resolution. This copy is not identical to the official copy.

I. Introduction

Wireless multicarrier (MC) communication systems utilize multiple complex exponentials as information-bearing carriers. MC transmissions thus retain their shape and orthogonality when propagating through linear time-dispersive media, precisely as eigen-signals do when they pass through LTI systems. They were first conceived and implemented with analog oscillators in the 60s [44], [73], but it was not until their all-digital implementation with the Fast Fourier Transform (FFT), that their attractive features were unraveled and sparked widespread interest for adoption in various single-user and multiple access (MA) communication standards [2]. Nowadays, MC systems such as the Orthogonal Frequency-Division Multiplexing (OFDM) are included in the Digital Audio/Video Broadcasting (DAB/DVB) standards in Europe [7], [12], [13], [39], [45], [48], [59] while the Discrete Multi-Tone (DMT), its wireline counterpart in the US, has been applied to high-speed Digital Subscriber Line (DSL) modems over twisted pairs [3], [6], [30]. OFDM has also been proposed for Digital Cable Television systems [50] and local area mobile wireless networks such as the IEEE802.11a, the MMAC and the HIPERLAN/2 [1], [8], [11], [14], [62]. MC hybrids with direct-sequence code division multiple access (DS-CDMA) spread-spectrum (SS) systems have also been developed for wideband cellular communications and proposed variations are known under acronyms such as OFDMA, MC-CDMA, MC-DS-CDMA, MT-CDMA and MC-SS-MA [15], [18], [25], [32], [40], [46], [63], [71]. Wideband CDMA is a strong contestant for third generation systems that include the International Mobile Telecommunications (IMT-2000) standard and the Universal Mobile Telecommunications System (UMTS) standard [42].

MC and DS-CDMA systems transmit information in blocks of Inverse FFT (IFFT) processed symbols and user-signature chips, respectively. And they both experience Inter-Block Interference (IBI) when their transmitted blocks propagate through LTI multipath channels because the underlying channel's impulse response combines contributions from more than one transmitted block at the receiver. To account for IBI, MC systems rely on the so called cyclic prefix (CP) which consists of redundant symbols replicated at the beginning of each transmitted block. To eliminate IBI, the redundant part of each block is chosen greater than the channel length and is discarded at both MC and DS-CDMA receivers in a fashion identical to that used in the overlap-save method of block convolution [43].

Prompted by such striking similarities, this paper takes a signals-and-systems viewpoint and lays out a systematic discrete-time equivalent matrix-vector model for block transmissions and their equalization (Section II), as they apply to single-user MC systems in general and OFDM in particular (Section III). The unifying framework encompasses CP-OFDM and novel alternatives that capitalize on transmit-redundancy [17], [52], [53]. It also highlights basic (albeit not widely acknowledged) advantages of block over serial equalization and it lends itself naturally to an all-digital implementation, unlike most existing formulations that rely on continuous-time MC models. As a by product, it will hopefully motivate further signal processing research in this exciting area of telecommunication systems.

MC and SS transmissions offer complementary strengths when it comes to coping with the idiosyncrasies of the wireless medium and its performance-limiting challenges that include: i)frequency-selective multipath propagation that manifests itself as a convolutive fading channel and causes intersymbol interference (ISI); ii) multi-user interference (MUI) that is responsible for near-far effects (high-power "nearby" users masking "weak" users located "far-away"); and iii)multiplicative (time-selective) fading effects that arise due to mobility and carrier offsets. Retaining their orthogonality through LTI systems, MC transmissions through multipath are MUI resilient, while DS-CDMA signaling requires multiuser detection [64] because convolutive fading destroys the orthogonality of user codes and may even render symbol recovery

This paper appeared in the IEEE Signal Processing Magazine, volume 17, number 3, pages 29–48, May 2000. This is a personal copy of it.

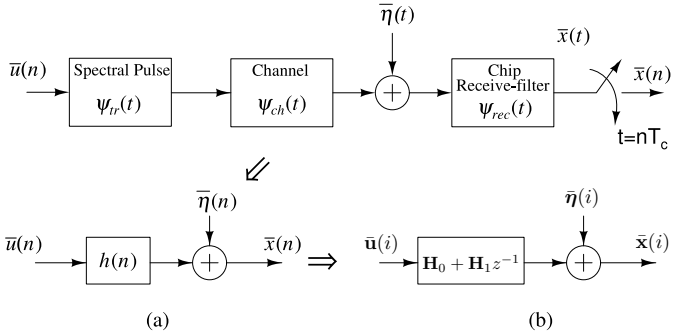

Fig. 1. Discrete-time channel a)serial; b)block with $P \geq L$

impossible [67]. On the other hand, by spreading information across the available bandwidth and coherently combining it at the receiver, DS-CDMA offers tolerance to multipath, whereas MC transmissions exhibit sensitivity to channel fades (LTI channel zeros on, or, close to carrier frequencies). To mitigate both MUI and convolutive fading and thereby improve their capacity and bit error rate (BER) performance, DS-CDMA and MC systems can either resort to error control codes at the expense of further expanding the precious bandwidth resource, or, join forces to complement their strengths. Section IV of this paper pursues the second option and develops a novel interpretation of the Generalized Multi-Carrier (GMC) CDMA approach, that was originally derived in [21], [22], [67], [69], relying solely on block symbol spreading and FFT operations. GMC-CDMA will prove to be MUI- and ISI-resilient and will be shown to guarantee symbol recovery regardless of the frequency-selective channel fades, and without sacrificing bandwidth efficiency – the only multiuser scheme possessing these attractive features for uplink transmissions (from the mobile users to the base station (BS)). The possibility to offer MC transmissions with virtually constant modulus and the capability to deliver multirate services for multimedia will also be stressed as they constitute important characteristics unique to GMC-CDMA.

Notation:: We will use bold capital (lower case) letters to denote matrices (column vectors), sometimes with subscripts to emphasize their sizes. An $N \times N$ identity matrix will be denoted as $\mathbf{I}_N$ and an all-zero matrix of size $K \times N$ will be denoted as $\mathbf{0}_{K\times N}$. We will use $\mathrm{E}[\cdot]$ to denote ensemble average, $\star$ for convolution, $\mathrm{tr}(\mathbf{B})$ for the trace of a matrix $\mathbf{B}$, $(\cdot)^{\mathcal{H}}$ for Hermitian transpose, $(\cdot)^{\dagger}$ for pseudo-inverse, and $\otimes$ for the Kronecker product. We will index the transmitted "chip sequence" by n. The information sequence will be referred to as symbols and i will denote block index for both symbol and chip blocks. The (k,l)th entry of a matrix $\mathbf{B}$ will be denoted as $[\mathbf{B}]_{k,l}$.

II. Block Transmission and Equalization

We will be concerned with digital wireless transmissions through linear time-invariant (LTI) discrete-time baseband equivalent channels. To create the link between a physical continuous-time channel and its discrete-time equivalent, consider the setup depicted in Figure 1. Sequence $\bar{u}(n)$ is analog-to-digital converted (not shown in the figure) and filtered by the spectral shaping pulse $\psi_{tr}(t)$. It then passes through the continuous-time dispersive channel $\psi_{ch}(t)$ and through the receive filter $\psi_{rec}(t)$. Let $h(t) := \psi_{tr}(t) \star \psi_{ch}(t) \star \psi_{rec}(t)$ denote the overall impulse response of the cascade: transmit-filter, continuous-channel, and receive-filter. The received baseband signal can then be written as $\bar{x}(t) = \sum_{\mu=-\infty}^{\infty} \bar{u}(n) h(t - nT_c) + \bar{\eta}(t) \star \psi_{rec}(t)$, where $\bar{\eta}(t)$ is the additive noise. With $\bar{x}(t)$ sampled at the chip rate $1/T_c$, the discrete-time received sequence defined as $x(n) := \bar{x}(t)\big|_{t=nT_c}$ is given by

$$\bar{x}(n) = \sum_{l=0}^{L} h(l)\bar{u}(n-l) + \bar{\eta}(n), \tag{1}$$

where $h(n) := h(t)\Big|_{t=nT_c}$ and $\bar{\eta}(n) := [\bar{\eta}(t) \star \psi_{rec}(t)]\Big|_{t=nT_c}$. In the sequel, we will only consider such simplified discrete-time equivalent channel models which will be assumed to satisfy:

Assumption 1: Sampled channels have finite impulse response (FIR) and their orders are no greater than L.

The order L is determined by dividing the maximum path delay (also known as maximum delay spread) with the sampling period (here equal to the chip duration T_c).

A. Blocking and IBI Suppression

For transmissions over wireless dispersive media, channel induced ISI is a major performance limiting factor. To mitigate such a time-domain dispersive effect that gives rise to frequency selectivity, it will prove useful to transmit the information-bearing chips in blocks. To be specific, we group the serial $\bar{u}(n)$ into blocks of size $P \gg L$ and correspondingly define the ith transmitted block to be $\bar{\mathbf{u}}(i) := [\bar{u}(iP), \bar{u}(iP+1), \ldots, \bar{u}(iP+P-1)]^T$ and the ith received as $\bar{\mathbf{x}}(i) := [\bar{x}(iP), \bar{x}(iP+1), \ldots, \bar{x}(iP+P-1)]^T$. Using (1), we can relate transmit- with receive- blocks as (see Figure 1b)

$$\bar{\mathbf{x}}(i) = \mathbf{H}_0 \bar{\mathbf{u}}(i) + \mathbf{H}_1 \bar{\mathbf{u}}(i-1) + \bar{\boldsymbol{\eta}}(i), \tag{2}$$

where $\bar{\boldsymbol{\eta}}(i)$ is the corresponding noise vector, and for $l = 0, 1$, the $P \times P$ matrices $\mathbf{H}_l$ are defined to have the (i,j)th entry as $h(lP + i - j)$; i.e.,

$$\mathbf{H}_0 = \begin{pmatrix} h(0) & 0 & 0 & \cdots & 0 \\ \vdots & h(0) & 0 & \cdots & 0 \\ h(L) & \cdots & \ddots & \cdots & \vdots \\ \vdots & \ddots & \cdots & \ddots & 0 \\ 0 & \cdots & h(L) & \cdots & h(0) \end{pmatrix}, \tag{3}$$

$$\mathbf{H}_1 = \begin{pmatrix} 0 & \cdots & h(L) & \cdots & h(1) \\ \vdots & \ddots & 0 & \ddots & \vdots \\ 0 & \cdots & \ddots & \cdots & h(L) \\ \vdots & \vdots & \vdots & \ddots & \vdots \\ 0 & \cdots & 0 & \cdots & 0 \end{pmatrix}. \tag{4}$$

Due to the dispersive nature of the channel, IBI arises between successive blocks, and renders $\bar{\mathbf{x}}(i)$ in (2) dependent on both $\bar{\mathbf{u}}(i)$ and $\bar{\mathbf{u}}(i-1)$.

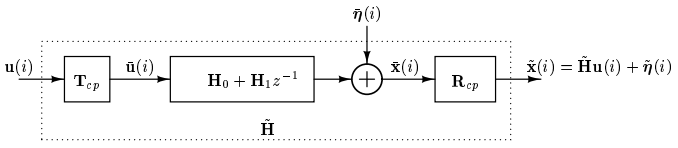

Fig. 2. Block transmission with cyclic prefix

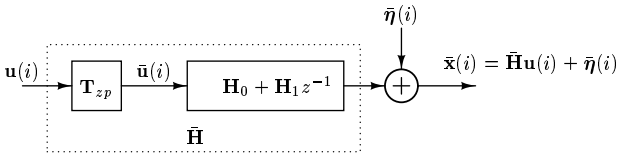

Fig. 3. General block transmission with zero-padding

If $\bar{\mathbf{x}}(i)$ blocks are IBI-free, then we can process them independently in an additive white Gaussian noise (AWGN) environment. To obtain IBI-free blocks, we need to introduce "guard chips" in the transmitted blocks $\bar{\mathbf{u}}(i)$. We start with an $N \times 1$ vector $\mathbf{u}(i)$ and create $\bar{\mathbf{u}}(i) = \mathbf{T}\mathbf{u}(i)$, where the guard-inserting matrix $\mathbf{T}$ is $P \times N$, with $P = N + L$. We can write (2) as

$$\bar{\mathbf{x}}(i) = \mathbf{H}_0\mathbf{T}\mathbf{u}(i) + \mathbf{H}_1\mathbf{T}\mathbf{u}(i-1) + \bar{\boldsymbol{\eta}}(i). \tag{5}$$

We observe that P symbols are now used to transmit $N := P - L$ symbols.

One has at least two options to obtain IBI-free transmissions of $\mathbf{u}(i)$, which we detail subsequently: Option 1) to simply discard the first L entries in the received block $\bar{\mathbf{x}}(i)$, or, Option 2) to zero-pad the transmitted block $\mathbf{u}(i)$ with L trailing zeros [17] by appropriately choosing $\mathbf{T}$.

Option 1: : To describe how the first L entries in $\bar{\mathbf{x}}(i)$ are discarded, we define the receive-matrix $\mathbf{R}_{cp} := [\mathbf{0}_{N\times L}\ \mathbf{I}_N]$. Pre-multiplying the received $\bar{\mathbf{x}}(i)$ by $\mathbf{R}_{cp}$ yields the IBI-free block $\tilde{\mathbf{x}}(i) := \mathbf{R}_{cp}\bar{\mathbf{x}}(i) = \tilde{\mathbf{H}}_0\mathbf{T}\mathbf{u}(i) + \tilde{\boldsymbol{\eta}}(i)$ (see Figure 2), where the $N \times P$ matrix $\tilde{\mathbf{H}}_0$ is the same as $\mathbf{H}_0$ with its first L rows removed; the noise vector $\tilde{\boldsymbol{\eta}}(i) := \mathbf{R}_{cp}\bar{\boldsymbol{\eta}}(i)$ holds the last N entries of $\bar{\boldsymbol{\eta}}(i)$. Note that the IBI-inducing matrix $\mathbf{H}_1$ has been eliminated by $\mathbf{R}_{cp}$ (one can verify by direct substitution from (4) that $\mathbf{R}_{cp}\mathbf{H}_1 = \mathbf{0}_{N\times P}$).

Discarding chips affected by IBI at the receiver has been widely used in OFDM standards and related MC transmissions, where the transmitted vector $\bar{\mathbf{u}}(i)$ contains a CP of length L: its pth entry is a replica of the $(p+N)$th entry, $p = 1, 2, \ldots, L$. The CP insertion can be described by choosing $\mathbf{T} = \mathbf{T}_{cp} := [\mathbf{I}_{cp}^T\ \mathbf{I}_N^T]^T$, which is a concatenation of the last L rows of an $N \times N$ identity matrix $\mathbf{I}_N$ (that we denote as $\mathbf{I}_{cp}$), and the identity matrix $\mathbf{I}_N$ itself.

To relate the IBI-free $\tilde{\mathbf{x}}(i)$ with $\mathbf{u}(i)$, we form $\tilde{\mathbf{H}}_0\mathbf{T}_{cp}$, and note that $\mathbf{T}_{cp}$ adds the first L columns of $\tilde{\mathbf{H}}_0$ to its corresponding last L columns, and thereby creates an $N \times N$ circulant matrix $\tilde{\mathbf{H}} := \tilde{\mathbf{H}}_0\mathbf{T}_{cp} = \mathbf{R}_{cp}\mathbf{H}_0\mathbf{T}_{cp}$ with its (k,l)th entry given by $h\big((k-l) \mod N\big)$. Using $\tilde{\mathbf{H}}$, we can describe the input-output relation in Figure 2 as

$$\tilde{\mathbf{x}}(i) = \tilde{\mathbf{H}}\mathbf{u}(i) + \tilde{\boldsymbol{\eta}}(i), \tag{6}$$

which shows that: by inserting (through the $\mathbf{T}_{cp}$ matrix) the CP at the transmitter and discarding it at the receiver (via matrix $\mathbf{R}_{cp}$), the linear convolutive channel with IBI in (2) is converted to a circular one without IBI. Such a conversion will be exploited in Section III to derive the well-known OFDM with CP. CP-OFDM relies also on the following important property of circulant matrices (see e.g., [24, p. 202]).

Fact 1: (Diagonalization of a circulant matrix) An $N \times N$ circulant matrix $\tilde{\mathbf{H}}$ can be diagonalized by pre- and post-multiplication with N-point FFT and IFFT matrices; i.e., $\mathbf{F}\tilde{\mathbf{H}}\mathbf{F}^{-1} = \mathbf{D}_H := \mathrm{diag}\big[H(e^{j0}), H(e^{j2\pi/N}), \ldots, H(e^{j2\pi(N-1)/N})\big]$, where $[\mathbf{F}]_{k,n} = N^{-\frac{1}{2}}\exp(-j2\pi kn/N)$ and $H(e^{j2\pi f}) := \sum_{n=0}^{L} h(n)\exp(-j2\pi fn)$ is the frequency response of the LTI channel.

Because the FFT (and thus its matrix $\mathbf{F}$) is invertible, we deduce that the circulant matrix $\tilde{\mathbf{H}}$ is invertible if and only $\mathbf{D}_H$ is invertible. Therefore, we have:

Fact 2: (Invertibility of a circulant matrix) The circulant channel convolution matrix $\tilde{\mathbf{H}}$ is invertible if and only if the channel transfer function has no zero on the FFT grid, i.e., $H(e^{j2\pi k/N}) \neq 0$, $\forall k \in [0, N-1]$.

Fact 2 will be used in Section II-B to identify conditions for symbol recovery in block transmission systems with CP. But for now, let us discuss the other option of eliminating IBI.

Option 2:: Note that if $\mathbf{T}$ in (5) is chosen so that $\mathbf{H}_1\mathbf{T} = \mathbf{0}_{P\times N}$, then IBI disappears. This corresponds to zero-padded (ZP) block transmissions[1] [17], [51]–[53]. In our matrix model, it amounts to setting the last L rows of $\mathbf{T}$ to zero, i.e., $\mathbf{T} = \mathbf{T}_{zp} := [\mathbf{I}_N^T\ \mathbf{0}_{L\times N}^T]^T$. Since only the last L columns of $\mathbf{H}_1$ in (2) are non-zero, it can be easily verified that $\mathbf{H}_1\mathbf{T}_{zp} = \mathbf{0}_{P\times N}$.

Forming the $P \times N$ matrix $\bar{\mathbf{H}} := \mathbf{H}_0\mathbf{T}_{zp}$ from the first N columns of matrix $\mathbf{H}_0$, we can write the received block $\bar{\mathbf{x}}(i)$ as (c.f. (2) and Figure 3)

$$\bar{\mathbf{x}}(i) = \bar{\mathbf{H}}\mathbf{u}(i) + \bar{\boldsymbol{\eta}}(i). \tag{7}$$

One special property of matrix $\bar{\mathbf{H}}$ in (7), not possessed by $\tilde{\mathbf{H}}$ in (6), is that its tall Toeplitz structure guarantees its full rank (it only becomes rank deficient when $h(n) = 0$, $\forall n \in [0, L]$, which means that the channel impulse response is identically zero, which is impossible in practice). Full rank of $\bar{\mathbf{H}}$ guarantees detectability of $\mathbf{u}(i)$ from $\bar{\mathbf{x}}(i)$ [17]. We will elaborate more on this aspect in Section II-B.

Up to now, we have seen two approaches to IBI-free transmission and reception described by the circular convolution model (6) and the linear model (7). Since circular convolution of two sequences is equivalent to their linear convolution followed by time-aliasing (see e.g., [43, p. 550]), we can proceed from (7) to obtain a circulant channel matrix $\tilde{\mathbf{H}}$ by adding the last L entries of $\bar{\mathbf{x}}(i)$ to the first L ones which implements the time-domain aliasing. In our block formulation, we define the time-aliasing matrix $\mathbf{R}_{zp} := [\mathbf{I}_N\ \mathbf{I}_{zp}]$, where $\mathbf{I}_{zp}$ consists of the first L columns of $\mathbf{I}_N$. Pre-multiplying a matrix or a vector by $\mathbf{R}_{zp}$ adds the last L rows to the first L rows, which we recognize as a matrix implementation of the overlap-add

[1] Similar to silent periods in TDMA, trailing zeros will not pose problems to high power amplifiers (HPA). And thanks to subsequent pulse-shaping, they will not give rise to out-of-band spectral leakage, either.

technique used in block convolution [43, p. 557]. Using this fact, one can verify that $\mathbf{R}_{zp}\bar{\mathbf{H}} = \tilde{\mathbf{H}}$ and write the time-aliased version of $\bar{\mathbf{x}}(i)$ as

$$\check{\mathbf{x}}(i) := \mathbf{R}_{zp}\bar{\mathbf{x}}(i) = \tilde{\mathbf{H}}\mathbf{u}(i) + \check{\boldsymbol{\eta}}(i), \tag{8}$$

where $\check{\boldsymbol{\eta}}(i) := \mathbf{R}_{zp}\bar{\boldsymbol{\eta}}(i)$ is the aliased noise. By comparing (6) with (8), we infer that starting from the linear convolution model (7), one can reach the circular model in (6) except for a slightly different noise vector. Bearing this in mind, we will consider henceforth only models (6) and (7), that we summarize in the following result (see also [17], [38], [52], [53], [72]):

Result 1: a) Blocking and IBI suppression with cyclic prefix: By inserting a CP of length L to the transmitted blocks $\mathbf{u}(i)$ through the matrix $\mathbf{T}_{cp}$, and then discarding the first L samples of each received block using the matrix $\mathbf{R}_{cp}$, we can convert the serial ISI channel $h(n)$ of order L to an IBI-free circular-convolution-based block system as in (6).
b) Blocking and IBI suppression with zero-padding: By zero padding each transmitted block $\mathbf{u}(i)$ with L trailing zeros, we can achieve IBI-free linear-convolution-based block transmission as in (7). By appropriate time-aliasing through $\mathbf{R}_{zp}$, (7) can be reduced to the circular-convolution-based block transmission system (8) as in the CP case.

B. Serial or Block Equalization?

So far, we have dealt with chip blocking and IBI suppression. By inserting redundant chips in the form of CP or ZP, we were able to achieve IBI-free reception. When it comes to equalization, such redundancy pays off. Let us first review briefly equalization of serial transmissions.

Serial equalization:: A serial equalizer of an LTI channel $h(n)$ with transfer function $H(z)$ is the LTI inverse system with transfer function $1/H(z)$. To avoid unbounded noise enhancement, we want the inverse system (if it exists) to be stable and also causal in order to reduce latency in equalization, which is sometimes critical for real-time applications. A causal and stable inverse of $h(n)$ exists only if $H(z)$ is minimum phase. If $H(z)$ has roots outside the unit circle, a stable inverse may still exist if we relax the causality requirement. When $H(z)$ has root(s) on the unit circle (that gives rise to channel fades), it is impossible to find a stable LTI inverse and linear serial equalization is impossible. Even when no zero lies exactly on the unit circle, the noise will still be enhanced at frequencies close to a channel fade and as a result, equalization performance will suffer. Since $h(n)$ is FIR, its inverse will have infinite impulse response (IIR). Therefore, an FIR channel can only be approximately equalized by an FIR equalizer obtained by truncating the IIR channel inverse.

Block equalization:: Let us now consider the block transmission models of Result 1. In the CP case, the received block $\tilde{\mathbf{x}}(i)$ is the circular convolution of the channel with the transmitted block $\mathbf{u}(i)$ (c.f. (6)). The circulant matrix $\tilde{\mathbf{H}}$ is not full rank when $H(z)$ has zero(s) on the FFT grid as asserted by Fact 2. In such cases, $\mathbf{u}(i)$ cannot be recovered from $\tilde{\mathbf{x}}(i)$ in general even when the channel $h(n)$ is known. In other words, recovery of $\mathbf{u}(i)$ from $\tilde{\mathbf{x}}(i)$ in the CP block transmission system (6) cannot be guaranteed for all FIR channels.

In the ZP case (7) however, since the matrix $\bar{\mathbf{H}}$ in (7) is always full rank, channel invertibility and thus symbol detectability is always guaranteed [17], [52]. Invertibility of ZP block transmissions holds true even when serial or CP block transmissions cannot be linearly equalized. Indeed, if $h(n)$ is known, we can obtain in the absence of noise the so-called zero-forcing (ZF) solution $\hat{\mathbf{u}}_{zf}(i)$ from $\bar{\mathbf{x}}(i)$ as [17], [51]:

$$\hat{\mathbf{u}}_{zf}(i) := \bar{\mathbf{H}}^{\dagger}\bar{\mathbf{x}}(i) := \mathbf{G}_{zf}\bar{\mathbf{x}}(i) = \mathbf{u}(i). \tag{9}$$

We call $\bar{\mathbf{H}}^{\dagger}$ a ZF equalizer for $\mathbf{u}(i)$ because it yields symbol estimation with zero ISI. In the presence of noise, $\hat{\mathbf{u}}_{zf}(i) = \mathbf{u}(i) + \bar{\mathbf{H}}^{\dagger}\bar{\boldsymbol{\eta}}(i)$ and the entries of $\bar{\mathbf{H}}^{\dagger}\bar{\boldsymbol{\eta}}(i)$ may have large variance if the condition number of $\bar{\mathbf{H}}^{\dagger}$ is large (it cannot be infinity though). To trade-off ISI for noise suppression, we may use the minimum mean square error (MMSE) equalizer $\mathbf{G}$ of size $N \times P$ that minimizes the MSE between $\mathbf{u}(i)$ and its estimate $\hat{\mathbf{u}}(i) := \mathbf{G}\bar{\mathbf{x}}(i)$. With correlation matrices $\mathbf{R}_u := \mathrm{E}[\mathbf{u}(i)\mathbf{u}^{\mathcal{H}}(i)]$ and $\mathbf{R}_{\bar{\eta}} := \mathrm{E}[\bar{\boldsymbol{\eta}}(i)\bar{\boldsymbol{\eta}}^{\mathcal{H}}(i)]$ assumed known, the MMSE receiver that minimizes $E \parallel \mathbf{u}(i) - \mathbf{G}\bar{\mathbf{x}}(i) \parallel^2$ is given by

$$\mathbf{G}_{mmse} = \mathbf{R}_u\bar{\mathbf{H}}^{\mathcal{H}}(\mathbf{R}_{\bar{\eta}} + \bar{\mathbf{H}}\mathbf{R}_u\bar{\mathbf{H}}^{\mathcal{H}})^{-1}. \tag{10}$$

Another important feature of ZP block transmission is its blind channel estimation capability [17], [53]. When both transmitted symbols and noise are white ($\mathbf{R}_u = \mathbf{I}_N$, $\mathbf{R}_{\bar{\eta}} = \sigma^2\mathbf{I}_P$), the autocorrelation matrix of the received block $\bar{\mathbf{x}}(i)$ is $\mathbf{R}_x = \bar{\mathbf{H}}\bar{\mathbf{H}}^{\mathcal{H}} + \sigma^2\mathbf{I}$. The first column of $\mathbf{R}_x$ is $[|h(0)|^2 + \sigma^2, h^*(0)h(1), \ldots, h^*(0)h(L), 0, \ldots, 0]^T$, which recovers all the channel coefficients (scaled by $h^*(0)$) except the first one [17]. If the noise variance is known, we can estimate all the channel coefficients to within the scale factor $h^*(0)$. This scale ambiguity is a feature of *all* blind channel estimation methods. Instead of the first column of $\mathbf{R}_x$, we may also consider the last column, which yields a channel estimate scaled by $h^*(L)$, except for the last entry that equals $|h(L)|^2 + \sigma^2$. Other subspace methods for blind channel estimation are also possible with ZP transmissions along the lines of [53]. Although blind channel estimation algorithms for CP transmission also exist, there are restrictions on the class of identifiable channels [37].

For the CP option, we can also define equalizers similar to (9) and (10). For example, a ZF equalizer to recover $\mathbf{u}(i)$ from (6) consists of an $N \times N$ matrix $\tilde{\mathbf{G}}_{zf} := \tilde{\mathbf{H}}^{-1}$, if the channel has no zero on the FFT grid. Although we may adopt an MMSE equalizer when the channel has zeros on (or close to) the FFT grid, lack of equalizability will introduce an error floor in the resulting BER performance. Nonlinear decision-feedback equalization offers a vital option but without linear (and often frequent) re-initialization it may lead to "run-away" effects due to error propagation especially at moderate to low SNR levels.

C. Post-, Pre-, or Balanced-Equalization?

We focus on ZF equalizers for the CP option to demonstrate the basic ideas. But MMSE (or other criteria for) equalization and the ZP option can be treated as well with minor modifications.

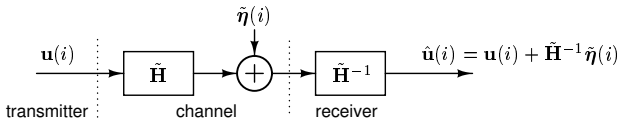

Fig. 4. Post equalization

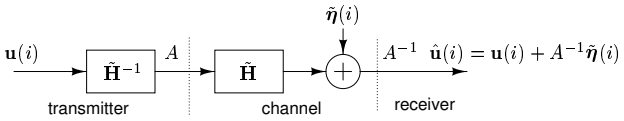

Fig. 5. Pre-equalization

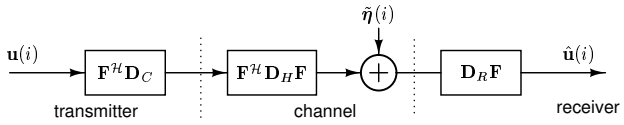

Fig. 6. Balanced equalization

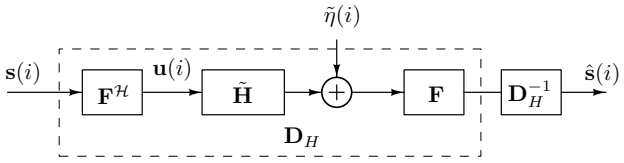

Fig. 7. Block diagram of CP-OFDM

Post-equalization:: Both (9) and (10) perform equalization of ZP transmissions *at the receiver* (hence the term *post-equalization*). Likewise, equalization of block transmissions with CP is accomplished also at the receiver by inverting (when possible) the square channel matrix $\tilde{\mathbf{H}}$ using $\tilde{\mathbf{G}}_{zf} = \tilde{\mathbf{H}}^{-1}$ (see (6) and Figure 4). If post-equalization is employed, the transmitter does not need access to *Channel State Information* (CSI). However, if the channel matrix is ill-conditioned, noise amplification might be unacceptably high. Let us suppose that both $\mathbf{u}(i)$ and $\tilde{\boldsymbol{\eta}}(i)$ are white with correlation matrices $\mathbf{R}_u = \mathbf{I}_N$ and $\mathbf{R}_{\tilde{\eta}} = \sigma^2\mathbf{I}_N$. The transmitted power is then $\mathrm{tr}(\mathbf{R}_u) = N$ and the total noise power is $\sigma^2_{post} := \mathrm{E}\,\|\tilde{\mathbf{H}}^{-1}\tilde{\boldsymbol{\eta}}(i)\|^2 = \sigma^2\,\mathrm{tr}\big(\tilde{\mathbf{H}}^{-1}\tilde{\mathbf{H}}^{-\mathcal{H}}\big)$.

In the ZP case, the channel matrix will be $\bar{\mathbf{H}}$ (instead of $\tilde{\mathbf{H}}$) with corresponding equalizer $\bar{\mathbf{H}}^{\dagger}$ (instead of $\tilde{\mathbf{H}}^{-1}$). The same noise enhancement problem appears, but not as severe as in the CP case because the matrix $\bar{\mathbf{H}}$ is always invertible.

Pre-equalization:: When the transmitter has access to CSI (e.g., through a feedback channel), one may alternatively consider placing the equalizing matrix $\tilde{\mathbf{H}}^{-1}$ *at the transmitter* to *pre-equalize* the block transmissions (c.f. Figure 5). With $\tilde{\mathbf{H}}^{-1}$ at the transmitter, we avoid the noise enhancement problem at the price of possibly having to transmit at higher power. In Figure 5, we have introduced a constant A at the transmitter to control the power of the transmitted block which is now $A\tilde{\mathbf{H}}^{-1}\mathbf{u}(i)$ instead of $\mathbf{u}(i)$. By choosing A such that $\mathrm{E}\,\|\,A\tilde{\mathbf{H}}^{-1}\mathbf{u}(i)\,\|^2 = \mathrm{E}\,\|\,\mathbf{u}(i)\,\|^2$, we can equate the transmit powers in pre- and post-equalization. Assuming whiteness of both $\mathbf{u}(i)$ and $\tilde{\boldsymbol{\eta}}(i)$ ($\mathbf{R}_u = \mathbf{I}_N$ and $\mathbf{R}_{\tilde{\eta}} = \sigma^2\mathbf{I}_N$), the amplitude $A = N^{\frac{1}{2}}\big[\mathrm{tr}(\tilde{\mathbf{H}}^{-1}\tilde{\mathbf{H}}^{-\mathcal{H}})\big]^{-\frac{1}{2}}$ will make the total transmitted power equal to N (as in the post-equalization) and the total receive noise power will now be $\sigma^2_{pre} := \mathrm{E}\,\|\,A^{-1}\tilde{\boldsymbol{\eta}}(i)\,\|^2 = \mathrm{tr}\big(\tilde{\mathbf{H}}^{-1}\tilde{\mathbf{H}}^{-\mathcal{H}}\big) = \sigma^2_{post}$. Although $\sigma^2_{pre} = \sigma^2_{post}$, the distribution of the total power among the entries of each noise vector is different, which may lead to different BER performance. Intuitively, pre-equalization is more appealing because it distributes the noise power evenly; but it requires CSI access at the transmitter. Often, the feedback channel for sending CSI may be noisy, or the channel variations may be too rapid, or the cost of estimating and feeding back CSI to the transmitter may be too high.

We also remark that related transmitter precoding ideas date back to Tomlinson and Harashima [26], [60] and have also been applied to multiuser communications in a downlink setup, where all users share the same additive white Gaussian noise (AWGN) channel (without multipath) [65].

Balanced equalization:: Combination of pre- and post-equalization is also possible. Since $\tilde{\mathbf{H}} = \mathbf{F}^{\mathcal{H}}\mathbf{D}_H\mathbf{F}$ (c.f. Fact 1), one can choose the transmitter to be $\mathbf{F}^{\mathcal{H}}\mathbf{D}_C$ and the receiver to be $\mathbf{D}_R\mathbf{F}$ (see Figure 6), where $\mathbf{D}_C$ and $\mathbf{D}_H$ are $N \times N$ diagonal matrices taking care of pre- and post-equalization, respectively. For example, with the ZF constraint $\mathbf{D}_R\mathbf{D}_H\mathbf{D}_C = \mathbf{I}_N$, one may choose $\mathbf{D}_C = A\mathbf{D}_H^{\frac{1}{2}}$ and $\mathbf{D}_R = A^{-1}\mathbf{D}_H^{-\frac{1}{2}}$, where A controls transmit power. It turns out that this choice of $\mathbf{D}_C$ and $\mathbf{D}_R$ minimizes the total after-equalization noise power $\sigma^2_{prepost} := \mathrm{E}\,\|\,\mathbf{D}_R\mathbf{F}\tilde{\boldsymbol{\eta}}(i)\,\|^2$ (i.e., $\sigma^2_{prepost} \le \sigma^2_{pre} = \sigma^2_{post}$), assuming the same transmit power and whiteness of $\mathbf{u}(i)$ and $\tilde{\boldsymbol{\eta}}(i)$. But similar to pre-equalization, balanced equalization requires CSI at the transmitter.

III. OFDM: Single User Multicarrier

It turns out that OFDM fits very well the block transmission setup we discussed so far and our formulation will suggest novel OFDM systems and related systems that are competitive to OFDM in some aspects and will lead us to important generalizations to multiuser systems in Section IV.

A. CP-OFDM

If the block transmitter with CP (Figure 6) does not have access to CSI, we can select $\mathbf{D}_C = \mathbf{I}$ so that the precoder in the balanced transceiver is only an IFFT matrix $\mathbf{F}^{\mathcal{H}}$ (see Figure 7). For ZF equalization, we choose the diagonal matrix at the receiver as $\mathbf{D}_R = \mathbf{D}_H^{-1}$; i.e., the receiver matrix is $\mathbf{D}_H^{-1}\mathbf{F}$. The resulting transmission scheme is called CP-OFDM and is illustrated in Figure 7; here, $\mathbf{s}(i) = [s(iN)s(iN+1)\ldots s(iN+N-1)]^T$ denotes the blocked information symbol sequence and $\mathbf{u}(i)$ now denotes its IFFT as $\mathbf{F}^{\mathcal{H}}\mathbf{s}(i)$.

Multicarrier Interpretation:: CP-OFDM belongs to the class of MC systems and was originally proposed for frequency multiplexing. To reveal the MC nature of CP-OFDM, we break the matrix-vector multiplication $\mathbf{u}(i) = \mathbf{F}^{-1}\mathbf{s}(i) = \mathbf{F}^{\mathcal{H}}\mathbf{s}(i)$ as

$$\mathbf{u}(i) = \sum_{k=0}^{N-1} \mathbf{f}_k s(i;k), \tag{11}$$

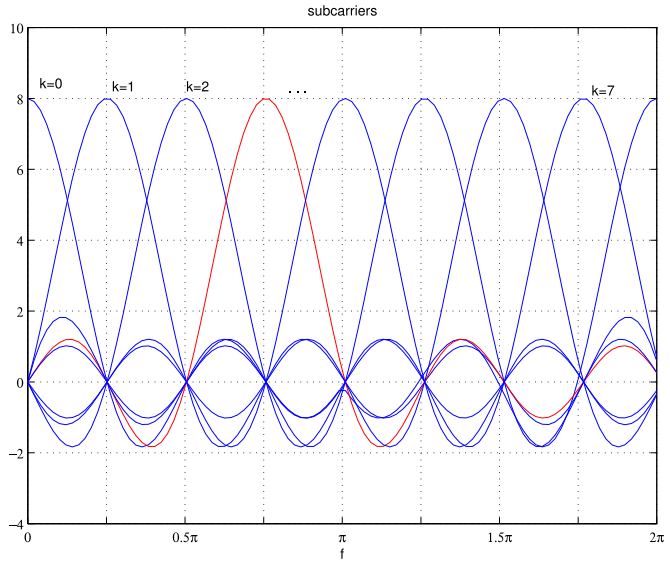

Fig. 8. Subcarriers in OFDM ($N = 8$)

where $\mathbf{f}_k := N^{-\frac{1}{2}}[\exp(j0), \exp(j2\pi k/N), \ldots, \exp(j2\pi k(N-1)/N)]^T$ is the kth column of the IFFT matrix $\mathbf{F}^{\mathcal{H}}$ and $s(i;k) := s(iN+k)$. Vectors $\mathbf{f}_k$ are finite duration discrete-time complex exponentials, representing sampled versions of the continuous carrier signals $\exp(j2\pi f_k t)$. It fact, the Discrete-Time Fourier transform (DTFT) of $\mathbf{f}_k$'s are sinc functions (see Figure 8). For this reason, we term vectors $\mathbf{f}_k$ and (sometimes $\exp(j2\pi k/N)$) as subcarriers.

Because complex exponentials are eigen-functions of LTI systems, $\mathbf{f}_k$'s are eigen-vectors of $\tilde{\mathbf{H}}$ (c.f. Fact 1). Such eigen-signals are only scaled by the channel's frequency response and yield the received block in the absence of noise as

$$\tilde{\mathbf{x}}(i) = \sum_{k=0}^{N-1} H(e^{j\frac{2\pi}{N}k})\mathbf{f}_k s(i;k). \tag{12}$$

When pre-multiplied by $\mathbf{f}_k^{\mathcal{H}}$, vector $\tilde{\mathbf{x}}(i)$ yields: $\tilde{x}(k) := \mathbf{f}_k^{\mathcal{H}}\tilde{\mathbf{x}}(i) = H(e^{j2\pi k/N})s(i;k)$, $k = 0, 1, \ldots, N-1$, which enables the low-complexity equalization (simple division), represented in Figure 7 by the matrix $\mathbf{D}_H^{-1}$.

Coded-OFDM:: Low complexity is certainly a strong motivation behind OFDM's widespread popularity, especially for high rate transmissions (experimental systems with transmission rates as high as 155 Mbps have been built [9]). But as we recall, equalization of CP-OFDM transmissions is only possible when the channel has no zero on the FFT grid so that the diagonal $\mathbf{D}_H$ matrix is invertible. If a sub-carrier frequency coincides with a channel null, then all the information carried by that subcarrier is lost. Channel coding together with interleaving and/or frequency hopping [49] may be used to cope with the "bad-subcarriers" in the so called coded OFDM (COFDM) variant at the price of reduced bandwidth efficiency (see e.g., [74]). In the worst case, to correct L errors induced by channel zeros, a linear block code must have a minimum Hamming distance $d_{\min} \geq 2L+1$. But for a block code with an input block of size k and an output block of size n, the Singleton bound asserts that $d_{\min} \leq n-k+1$ [55]. Therefore, at least $n-k = 2L$ redundant symbols must be transmitted. If we also consider the length-L CP inserted at the transmitter, a redundancy of at least $3L$ symbols is indispensable.

Channel Identification:: To perform the low-complexity equalization, the OFDM receiver needs to acquire CSI, e.g., by training, which consists of transmitting symbols (known to the receiver) periodically to enable channel estimation at the receive-end. Training based channel estimation has been adopted in the IEEE standard 802.11 [1], [8] and the European standard for HIPERLAN [11], [14]. Knowing training symbols $s(i;k)$ at the receiver, a channel estimator simply forms $\hat{H}(e^{j2\pi k/N}) = \tilde{x}(k)/s(i;k)$. Since the channel is assumed FIR of order $\leq L$, frequency responses at $L+1$ points suffice for channel identification. But sending training symbols at more frequencies improves channel estimation quality at the cost of expanding bandwidth or lowering the information rate.

To avoid bandwidth-consuming training sequences, blind channel estimators have also been devised for CP-OFDM systems. Some of them rely on the redundancy that is inherent to CP-OFDM transmissions in the form of CP [27], [37]. But they do not guarantee identifiability for all possible channels. A recently proposed blind channel estimator [72] capitalizes on the finite alphabet property of $s(i;k)$ to guarantee channel identifiability regardless of channel zero locations with minimal received data (PSK signals are recoverable even from a single OFDM block).

Discrete Multitone (DMT):: In DSL and Digital Cable TV systems, the channel does not vary very often and it is possible for the transmitter to acquire CSI from the receiver through feedback. Transmission in the so-termed Discrete Multitone (DMT) systems can be optimized according to certain criteria as we alluded to in Section II-C. Two key features of DMT are power loading and bit loading. Power loading consists of distributing power on (by varying the amplitudes of) different subcarriers. In our setup, power loading amounts to choosing the $\mathbf{D}_C$ matrix (c.f. Figure 6). For example, the $(k,k)th$ entry d_{kk} of a $\mathbf{D}_C^{\text{opt}}$ matrix that maximizes information rate between $\mathbf{u}(i)$ and $\tilde{\mathbf{x}}(i)$ for a prescribed transmit power $\mathcal{P}_0 := \sum_{k=0}^{K-1} |d_{kk}|^2$ is given by [51]:

$$|d_{kk}|^2 = \begin{cases} \lambda - \frac{\sigma^2}{|d_{H,k}|^2}, & \text{if } \lambda > \frac{\sigma^2}{|d_{H,k}|^2} \\ 0, & \text{otherwise,} \end{cases} \tag{13}$$

where $d_{H,k} := [\mathbf{D}_H]_{k,k}$ and λ is chosen to satisfy the prescribed power (we have assumed that $\mathbf{u}(i)$ and $\bar{\boldsymbol{\eta}}(i)$ are Gaussian and white $\mathbf{R}_u = (1/\sigma^2)\mathbf{R}_{\bar{\eta}} = \mathbf{I}$). If they are colored, pre-whitening techniques can be applied [51]. Thanks to the diagonalization, each subcarrier can be viewed as a separate AWGN channel, on which different number of bits can be loaded to achieve a specified BER performance using e.g., quadrature amplitude modulation (QAM) of different size per subchannel. The number of bits on the kth subcarrier can be approximated by [4]:

$$b_k = \log_2\left(1 + \frac{\text{SNR}_k}{\gamma}\right),$$

where $\text{SNR}_k := |d_{kk}d_{H,k}|^2/\sigma^2$ and γ is the "SNR-gap" between Shannon's channel capacity limit and the SNR required

for uncoded QAM. At BER=10^{-7}, γ is equal to 10 dB [4]. Recall that the capacity-maximizing input is Gaussian distributed on each subcarrier, while in practice finite-alphabet constellations are used. Also, the optimization in (13) is non-trivial and different loading algorithms for finite-alphabet constellations as well as low complexity suboptimum searches can be found in [5], [28], [51], [54].

B. ZP-OFDM

As we discussed in Section II-A, ZP can also achieve IBI-free reception [17], [38], [52], [53]. In ZP-OFDM, the transmitted sequence $\mathbf{u}(i)$ in (7) is chosen to be $\mathbf{F}^{\mathcal{H}}\mathbf{s}(i)$; therefore, the received block is $\bar{\mathbf{x}}(i) = \bar{\mathbf{H}}\mathbf{F}^{\mathcal{H}}\mathbf{s}(i) + \bar{\boldsymbol{\eta}}(i)$. Since $\mathbf{F}$ is full-rank, blind recovery of $\mathbf{u}(i)$ from $\bar{\mathbf{x}}(i)$ (c.f. Section II-B) also guarantees uniqueness in recovering information symbols $\mathbf{s}(i)$ blindly. This is precisely ZP-OFDM's edge over CP-OFDM [52]. That is, with the same amount of redundancy (L trailing zeros versus length-L cyclic prefix in CP-OFDM), ZP-OFDM guarantees symbol recovery for any Lth-order FIR channel.

As we mentioned in Section II-A, block transmissions with ZP can also be brought to a circular convolution model (c.f. (8)) by adding the last L samples in the received block to the first L samples. The low complexity CP-OFDM receiver is thus also applicable to ZP-OFDM, at the price of sacrificing symbol recovery guarantees [38]. Several equalization alternatives have been developed to restore symbol recovery with reduced-complexity in ZP-OFDM [38]. Similar to CP-OFDM, if CSI is available at the transmitter, the transmission can be optimized as in DMT using power- and bit-loading techniques [51].

If CSI is not available at the transmitter, OFDM transmissions are still well motivated thanks to their low equalization complexity at the FFT-based receiver. But if the receiver can afford a little extra complexity, one may be willing to modify the OFDM transmissions to gain in other aspects such as lowering the back-off levels in power amplification.

C. CP- and ZP-only

Part of the price one pays for the low complexity equalization in CP-OFDM and related MC schemes is high peak-to-average power ratio (PAR) due to the IFFT taken at the transmitter: the IFFT $\mathbf{u}(i) = \mathbf{F}^{\mathcal{H}}\mathbf{s}(i)$ of the input block $\mathbf{s}(i)$ may exhibit large amplitude variation from entry to entry even when $\mathbf{s}(i)$ entries have constant modulus (CM). Large PAR necessitates backing-off the HPA to avoid non-linear distortions. PAR reduction techniques increase the efficiency of HPAs and have been studied for the non-constant modulus OFDM transmissions (see e.g., [58], [70]).

Another possibility for reducing PAR, is to remove the IFFT altogether and transmit $\mathbf{u}(i) = \mathbf{s}(i)$ with either CP or ZP. We call the former CP-only and the latter ZP-only because only CP or ZP is introduced before transmission to assure IBI-free reception. The received block can be modeled by (6) in the CP case, or by (7) in the ZP case, with $\mathbf{u}(i)$ being replaced by $\mathbf{s}(i)$. Such CP or ZP operations have minimal effect on the PAR: if $\mathbf{s}(i)$ have CM, the transmitted block will also has CM except during the last L trailing zeros in ZP.

Let us now check equalization complexity with CP- or ZP-only transmissions. Since the ZP model (7) can be reduced to a circular one (c.f. (8)), it suffices to check CP-only. To equalize the circulant channel matrix $\tilde{\mathbf{H}}$ and recover the symbols $\mathbf{s}(i)$, we need to find $\tilde{\mathbf{H}}^{-1}$. But $\tilde{\mathbf{H}}^{-1} = \mathbf{F}^{\mathcal{H}}\mathbf{D}_H^{-1}\mathbf{F}$ according to Fact 1. We thus need to: i) perform FFT on the received block; ii) divide the result by the inverse of the channel frequency response (assuming there is no zero on the FFT grid); and iii) perform an IFFT to recover all symbols. Compared to CP-OFDM, which needs one FFT at the receiver plus scalar divisions, the CP-only (or ZP-only) scheme will need only one extra IFFT at the receiver. We have in essence "moved" the IFFT from the CP-OFDM transmitter to the receiver. With low PAR guaranteed, CP-only and ZP-only have the same transceiver complexity as CP-OFDM or ZP-OFDM. But since no subcarriers are used in transmitting $\mathbf{s}(i)$, when CSI is available at the transmitter, its optimization is not as direct as in DMT, where independent subcarriers can be power- and bit-loaded.

IV. Block-Spread Multiuser Multicarrier

Having discussed MC transmissions for single user systems, we now turn our attention to the wireless multiuser setup. We will focus on the uplink because the downlink can be viewed as a special case with each user receiving the aggregate BS transmission through a single channel.

A. Motivation

MUI and ISI constitute major limiting factors to BER performance and system capacity measured by the number of users that can be supported and their data rates [23]. Ideally, our goal is to eliminate MUI and ISI in order to guarantee symbol recovery with maximum possible bandwidth efficiency. Low complexity, flexibility, and capability to support multiple rates are also among the most desirable features. To achieve these (perhaps conflicting) objectives or a balanced trade-off among them, MC transmission combined with symbol blocking will prove to be a fruitful direction. We will argue first that receiver design alone is not sufficient for symbol recovery and MUI elimination purposes.

Many multiuser detection schemes have been developed (see e.g., [41], [64] and references therein). In the linear class, we have single user matched filters, decorrelating and MMSE receivers. Nonlinear multiuser detectors include successive interference cancelers, multistage, decision-feedback and maximum likelihood options. A number of (non-) blind CDMA receivers have also attempted to mitigate multipath effects [16], [34], [61]. However, it is not widely acknowledged that channel dispersion may render user symbols undetectable no matter how the receiver is designed. For example, suppose there are two users in an uplink DS-SS system. The first user's spreading sequence, channel, and transmitted symbol are $c_0(n) = \delta(n) + \delta(n-1) - \delta(n-2) - \delta(n-3)$, $h_0(n) = \delta(n) - \delta(n-1)$, and $+1$, respectively. Likewise, suppose that the second user has $c_1(n) = \delta(n) - \delta(n-1) - \delta(n-2) + \delta(n-3)$, $h_1(n) = \delta(n) + \delta(n-1)$ and -1, respectively. The received sequence will therefore be $(+1)\cdot$

$h_0(n) \star c_0(n) + (-1) \cdot h_1(n) \star c_1(n) \equiv 0$, an all-zero sequence from which the users' two symbols cannot be recovered. The users' spreading sequences are length-4 Walsh-Hadamard sequences, and thus orthogonal by design. In the presence of multipath, the resulting signature sequences are obtained by convolving the spreading codes with the corresponding channels. In this example, the channels have destroyed the orthogonality of the codes; indeed, the resulting signature sequences are linearly dependent. Lack of detectability can be a systematic problem that is inherent to the multipath-distorted received signal and cannot be removed through (even nonlinear) receiver designs. In multiuser detection terms, multipath may drive the asymptotic multiuser efficiency [64, p. 121] to 0 because the BER can be non-zero even in the absence of (thermal or sensor) noise.

B. Generalized MC (GMC) CDMA Principles

To assure symbol recovery in the presence of multipath, we need extra degrees of freedom that become available by judiciously designing not only our receivers but also our transmitters. Specifically, we will seek MUI/ISI eliminating transceivers for any FIR channel. We would also like the transmissions to be bandwidth efficient and transparent to multipath channels. Suppose there are M users in the system and that the class of channels satisfies:

Assumption 2: All users' channels include quasi-synchronism among users and are FIR of order $\leq L = \tilde{L} + D$, where $\tilde{L}$ is the maximum order (delay spread) of the chip-sampled multipath channels, and D is the maximum relative asynchronism among the users. Specifically, user μ's transfer function is assumed to be: $H_\mu(z) = z^{-d_\mu} \sum_{n=0}^{\tilde{L}} h_\mu(n) z^{-n}$, for some $d_\mu \in [0, D]$.

Quasi-synchronism supposes that users attempt to synchronize with the BS's pilot signal. Hence, they are not totally asynchronous and they are allowed to be off by a few chips that account for relative delays and clock synchronization errors [10]. Apart from having orders bounded by L, there is no restriction on where the FIR channel nulls are located.

GMC-CDMA relies on FDMA-like principles for channel-independent MUI elimination. In FDMA, the users transmit over non-overlapping frequency bands (see Figure 9 for two users). Since convolutive channels are multiplicative in the frequency domain, received FDMA transmissions will still occupy non-overlapping frequencies and can thus be separated by (often analog) filtering. Orthogonal FDMA (OFDMA), e.g., [40], [71], allows users' bands to overlap and retains FDMA-like orthogonality among the discrete-time subcarriers. In OFDMA, each user's symbol is sent on one individual subcarrier and will be lost if the user's channel happens to have a null at the subcarrier frequency. OFDMA systems often rely on channel coding techniques and/or frequency hopping to mitigate frequency-selective fading effects at the expense of possibly considerable bandwidth overexpansion.

One approach is to load the same symbol to more than L subcarriers, which guarantees that at least one subcarrier will survive the channel nulls. Although simple, this option is not appealing because it entails L-fold bandwidth increase.

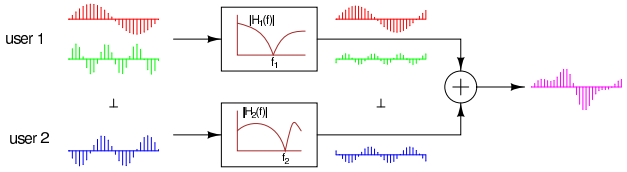

Fig. 9. Illustration of Multiuser MC system

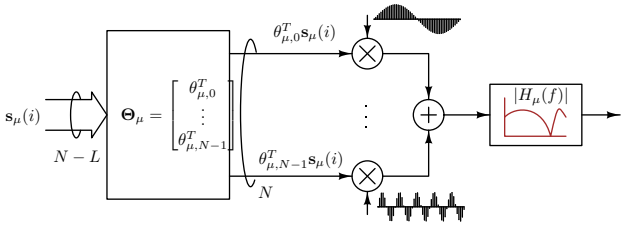

Fig. 10. Blocking and precoding of K symbols

Our remedy to the symbol recovery problem without bandwidth over-expansion is through *symbol blocking* and wisely introduced transmit-redundancy (see Figure 10). The idea is to let each user send $K \geq 1$ symbols jointly using $J \geq K$ subcarriers, instead of putting each of the K symbols on a separate subcarrier. The users' subcarriers are still kept distinct: each subcarrier will only be used by one user to allow for FDMA-like user separation in the frequency domain. To eliminate ISI and guarantee symbol recovery, we will linearly precode each user's block of K symbols to J symbols that we will place on J subcarriers so that all K symbols in the block are recoverable from any $J - L$ of the J subcarriers. That way, even if L of the J subcarriers are "hit" by channel nulls, the K symbols will "survive". For M user systems, the total number of subcarriers required is therefore $N = MJ$, and correspondingly we consider transmitting chips in blocks of N (recall that in OFDM systems, the number of subcarriers is the same as the size of the circulant channel matrix).

We stress that the linear precoders (matrices $\mathbf{\Theta}_\mu$ in Figure 10) have entries taking values in the complex field (instead of the Galois field[2]). This generalization is a powerful one, because it allows us to cope with unknown channels without sacrificing bandwidth, as we shall see in the next section.

Need for transmit redundancy:: We also want to reiterate that when it comes to estimating and equalizing frequency-selective channels with training or blindly, transmit-redundancy is indispensable. Indeed, training symbols (or pilots) needed for channel estimation constitute the transmit-redundancy in non-blind methods since they replace information symbols. Likewise, blind channel estimators relying on second-order statistics of fractionally-sampled received data will fail, unless sufficient excess bandwidth (and thus transmit-redundancy) is introduced. Higher-order blind methods (such as the CMA) rely on non-Gaussianity and are thus destined (by Shannon's Capacity Theorem) to transmit below the maximum possible rate that is achievable by Gaussian transmissions.

[2]Even in single user COFDM system, the coded block is inverse Fourier transformed and sent over a single physical carrier in a serial fashion. The need to keep the Galois field intact is no longer critical.

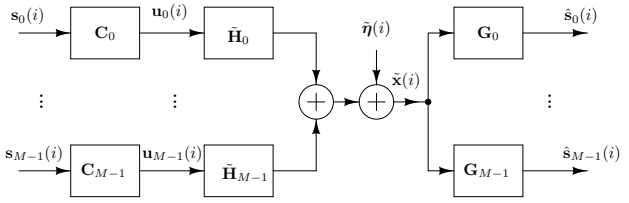

Fig. 11. Block model for block spreading system

Since *transmit-redundancy is a must when frequency selectivity is present*, it is meaningful to look for optimum means of introducing it. Our single-user comparisons in [53], [54] and multiuser results in [22], [67] and herein, support the view that the most flexible and bandwidth-efficient means of transmit-redundancy is realized by symbol blocking and precoding (block spreading).

C. GMC-CDMA Design

Similar to OFDM, we adopt block transmissions: the transmitted sequences are grouped in blocks of size $P = N+L$ that include either length-L CP or length-L ZP for IBI cancellation. For simplicity, we focus on the CP case, bearing in mind though that ZP can also be reduced to CP as per Result 1b). The μth user's channel will be represented as an $N \times N$ circulant matrix $\tilde{\mathbf{H}}_\mu$ (see (6) and Figure 11). Defining $\mathbf{C}_\mu$ to be user μ's $N \times K$ spreading (precoding) matrix, we can write user μ's transmitted $N \times 1$ vector as $\mathbf{u}_\mu(i) = \mathbf{C}_\mu \mathbf{s}_\mu(i)$. The received $N \times 1$ vector $\tilde{\mathbf{x}}(i)$ and the μth user's $K \times 1$ block-symbol estimate $\hat{\mathbf{s}}_\mu(i)$ can be written respectively as [18], [67]:

$$\tilde{\mathbf{x}}(i) = \sum_{\mu=0}^{M-1} \tilde{\mathbf{H}}_\mu \mathbf{C}_\mu \mathbf{s}_\mu(i) + \tilde{\boldsymbol{\eta}}(i), \quad \hat{\mathbf{s}}_\mu(i) = \mathbf{G}_\mu \tilde{\mathbf{x}}(i), \quad (14)$$

where $\mathbf{G}_\mu$ is user μ's $K \times N$ receive matrix.

Such a model is general enough to describe many DS-CDMA systems, as well as MC-DS hybrids including MC-CDMA, MC-DS-CDMA, MT-CDMA, MC-SS-MA. This is one reason we term our block model depicted in Figure 11 as generalized multicarrier (GMC) CDMA.

MUI-free multicarrier design:: Let us consider $\mathcal{F} := \{\exp(j2\pi l/N), l = 0, 1, \ldots, N-1\}$ to be the set of $N = MJ$ subcarriers (FFT frequencies) available to all users. Similar to Section III, we refer to the lth frequency $\exp(j2\pi l/N)$ as subcarrier l. Let $\{\mathcal{F}_\mu\}_{\mu=0}^{M-1}$ be a partitioning of $\mathcal{F}$ into M non-intersecting subsets, each of which contains J distinct subcarriers; i.e., with $\emptyset$ denoting the empty set, we have

$$\bigcup_{\mu=0}^{M-1} \mathcal{F}_\mu = \mathcal{F}, \quad \mathcal{F}_\mu \bigcap \mathcal{F}_m = \emptyset, \quad \forall \mu \neq m. \quad (15)$$

Subset $\mathcal{F}_\mu$ contains user μ's J subcarriers that we should henceforth view as the *signature subcarriers* of user μ. We denote the jth signature subcarrier of user μ by $\rho_{\mu,j}$, $j \in [0, J-1]$.

To unravel the attractive features of MUI/ISI-resilience progressively, we factor our spreading and despreading matrices $\{\mathbf{C}_\mu, \mathbf{G}_\mu\}_{\mu=0}^{M-1}$ in the following trilinear forms:

$$\mathbf{C}_\mu = \mathbf{F}^{\mathcal{H}} \boldsymbol{\Phi}_\mu \boldsymbol{\Theta}_\mu, \qquad \mathbf{G}_\mu = \boldsymbol{\Gamma}_\mu \boldsymbol{\Phi}_\mu^T \mathbf{F}, \quad (16)$$

with each matrix-factor playing a different role: $\boldsymbol{\Theta}_\mu$ is a $J \times K$ matrix that maps linearly the K information symbols of the ith block $\mathbf{s}_\mu(i)$ to J symbols $\boldsymbol{\Theta}_\mu \mathbf{s}_\mu(i)$; through an $N \times J$ subcarrier-selector matrix $\boldsymbol{\Phi}_\mu$, the latter is mapped to user μ's J signature subcarriers to obtain $\boldsymbol{\Phi}_\mu \boldsymbol{\Theta}_\mu \mathbf{s}_\mu(i)$. The (p,q)th entry of $\boldsymbol{\Phi}_\mu$ is 1 if $\rho_{\mu,q}$ is selected to be the pth subcarrier from $\mathcal{F}$ (i.e., if $\rho_{\mu,q} = \exp(j2\pi p/N)$), and 0 otherwise. In other words, the 0-1 entries of matrix $\boldsymbol{\Phi}_\mu$ determine (and are defined by) the subcarriers allocated to user μ. The user-independent IFFT matrix $\mathbf{F}^{\mathcal{H}}$ implements an OFDM modulation at the final stage. At the receiver, $\mathbf{F}$ performs FFT of the received vector $\tilde{\mathbf{x}}(i)$ and $\boldsymbol{\Phi}_\mu^T$ extracts user μ's J precoded symbols from the $N = MJ$ subcarriers (recall that user μ occupies J out of MJ subcarriers). Finally, the $K \times J$ matrix $\boldsymbol{\Gamma}_\mu$ equalizes the channel-precoder combination.

Forming $\hat{\mathbf{s}}_\mu(i) = \mathbf{G}_\mu \tilde{\mathbf{x}}(i)$, we can write the μth user's symbol estimates as (c.f. (16) and (14)):

$$\hat{\mathbf{s}}_\mu(i) = \boldsymbol{\Gamma}_\mu \sum_{m=0}^{M-1} \boldsymbol{\Phi}_\mu^T \mathbf{F} \tilde{\mathbf{H}}_m \mathbf{F}^{\mathcal{H}} \boldsymbol{\Phi}_m \boldsymbol{\Theta}_m \mathbf{s}_m(i) \quad (17)$$

$$+ \boldsymbol{\Gamma}_\mu \boldsymbol{\Phi}_\mu^T \mathbf{F} \tilde{\boldsymbol{\eta}}(i). \quad (18)$$

To eliminate MUI from (17), we rely on the following three properties:

p1) As per Fact 1, $\mathbf{F}\tilde{\mathbf{H}}_m\mathbf{F}^{\mathcal{H}}$ is an $N \times N$ diagonal matrix $\tilde{\mathbf{D}}_m := \mathrm{diag}[H_m(e^{j0}), \ldots, H_m(e^{j2\pi(N-1)/N})]$.

p2) Since $\boldsymbol{\Phi}_m$ has only a single non-zero unity entry per column, it can be readily verified that $\tilde{\mathbf{D}}_m \boldsymbol{\Phi}_m = \boldsymbol{\Phi}_m \mathbf{D}_m$, where $\mathbf{D}_m := \mathrm{diag}[H_m(\rho_{m,0}), \ldots, H_m(\rho_{m,J-1})]$ holds on its diagonal the frequency response of the mth user's channel sampled at the mth user's signature subcarriers.

p3) Thanks to the non-overlapping frequency allocation in (15), the corresponding subcarrier selector matrices $\boldsymbol{\Phi}_\mu$ are mutually orthogonal by construction; i.e., with $\delta(\cdot)$ denoting Kronecker's delta, we have:

$$\boldsymbol{\Phi}_\mu^T \boldsymbol{\Phi}_m = \delta(\mu - m) \mathbf{I}_J. \quad (19)$$

Based on p1)–p3), we can simplify (17) as

$$\hat{\mathbf{s}}_\mu(i) = \boldsymbol{\Gamma}_\mu \left[\mathbf{D}_\mu \boldsymbol{\Theta}_\mu \mathbf{s}_\mu(i) + \boldsymbol{\Phi}_\mu^T \mathbf{F} \tilde{\boldsymbol{\eta}}(i) \right] := \boldsymbol{\Gamma}_\mu \tilde{\mathbf{x}}_\mu(i), \quad (20)$$

where the quantity inside the square brackets is the $J \times 1$ MUI-free vector $\tilde{\mathbf{x}}_\mu(i)$ corresponding to user μ. From (17) to (20), we recognize how MUI is eliminated deterministically regardless of the multipath channels. Further, if $\tilde{\boldsymbol{\eta}}(i)$ is white with $\mathbf{R}_{\tilde{\eta}} = \sigma^2 \mathbf{I}_N$, the vectors $\boldsymbol{\Phi}_\mu^T \mathbf{F} \tilde{\boldsymbol{\eta}}(i)$ are also white and uncorrelated for different μ's due to the mutual orthogonality (19) and the orthonormality of the FFT matrix $\mathbf{F}$. The latter implies that if $\tilde{\boldsymbol{\eta}}(i)$ is also Gaussian, a single user optimum detector (or equalizer) following the MUI elimination step will also be optimum in our multiuser setup. In other words, our GMC-CDMA transceiver design in (16) has rendered the *multiple access channel equivalent to independent parallel single user frequency-selective channels with AWGN*. Following the MUI elimination step, the matrix $\boldsymbol{\Gamma}_\mu$ will (linearly)

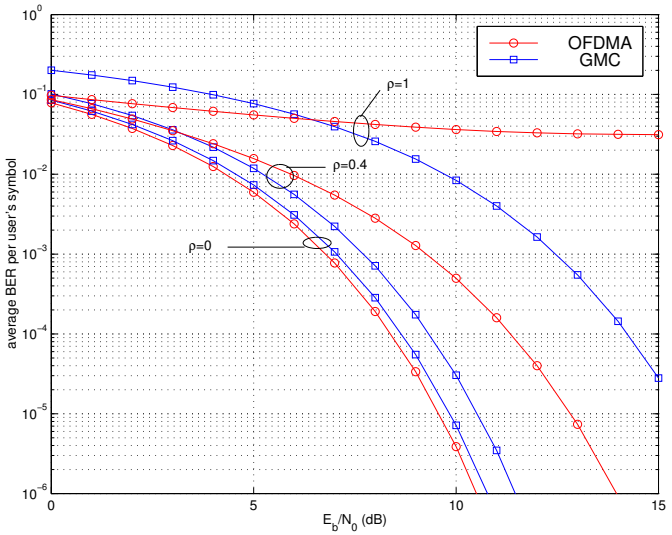

Fig. 12. Importance of symbol detectability

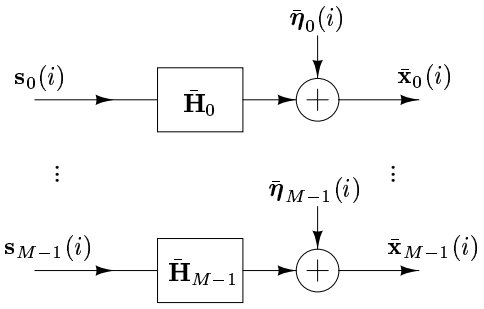

Fig. 13. MIMO to SISO equivalence

equalize the single-user ISI channel. Our MUI/ISI-resilient designs do not require knowledge of the system input (e.g., the constellation type) and as such they are also applicable to multichannel separation problems entailing signals from continuous amplitude distributions. Non-linear equalizers (e.g., ML and DFE) may also be considered to capitalize on the finite alphabet property of the information symbols [20], [57].

Symbol detectability:: In order to guarantee detectability of the K symbols in $\mathbf{s}_\mu(i)$ regardless of the signal constellation, we need the matrix $\mathbf{D}_\mu\mathbf{\Theta}_\mu$ in (20) to be full column rank, regardless of the μth channel. Hence, we require

$$\text{rank}(\mathbf{D}_\mu\mathbf{\Theta}_\mu) = K, \quad \forall \mu \in [0, M-1]. \tag{21}$$

If (21) holds, ZF equalization based on $\mathbf{\Gamma}_\mu = (\mathbf{D}_\mu\mathbf{\Theta}_\mu)^\dagger$ will then recover $\hat{\mathbf{s}}_\mu(i)$ as in (20). Constellation-independent symbol detectability offers great flexibility in selecting user constellations, which can be utilized by users to transmit at different data rates by adopting appropriate (e.g., QAM) constellation sizes and hence different bit loading schemes.

As per Assumption 2, each user's channel can have at most L zeros. Therefore, $\mathbf{D}_\mu$ can have at most L zero diagonal entries. For (21) to hold true for all channels satisfying Assumption 2, we thus need: *any* $J - L = K$ *rows of* $\mathbf{\Theta}_\mu$ *to be linearly independent*. Notice that this is not a condition on the channels but instead it is a guideline for designing $\mathbf{\Theta}_\mu$. A special choice of $\mathbf{\Theta}_\mu$ that satisfies this condition has entries

$$[\mathbf{\Theta}_\mu]_{l+1,k+1} = A_\mu \rho_{\mu,l}^{-k}, \tag{22}$$

where A_μ controls user μ's power. Matrix $\mathbf{\Theta}_\mu$ is Vandermonde and any K rows of it will form a full rank $K \times K$ matrix since they are Vandermonde vectors constructed from distinct signature frequencies.

Example 1: To emphasize the importance of guaranteed symbol recovery, we compare OFDMA with GMC-CDMA. We assumed $M = 16$ users in the downlink (a common two-ray channel) with $L = 1$ zero at $z = \rho$. For GMC-CDMA, we choose $K = 16$ (the number of information symbols in each block, that is not necessarily the same as M); precoder $\mathbf{\Theta}_\mu$ as in (22); and the user signature frequencies equally spaced and interleaved around the unit circle. We depict in Figure 12 the average BER of the two systems when $\rho = 0,\ 0.4$, and 1, respectively. When $\rho = 1$ (channel null on the FFT grid), one user in the OFDMA system will suffer consistently, which explains the error floor in the average BER curve. In contrast, GMC-CDMA shows no BER floor although it is also affected by frequency-selective fading. Also, even when $\rho = 0.4$, where both systems have no symbol detectability problem, GMC-CDMA performs better thanks to its built-in robustness against frequency-selective fading.

MIMO to SISO:: In addition to satisfying (21), it turns out that our precoder choice in (22) offers extra advantages. Forming $\mathbf{\Theta}_\mu\mathbf{s}_\mu(i)$ with $\mathbf{\Theta}_\mu$ as in (22) evaluates the DTFT of $\mathbf{s}_\mu(i)$ at the user μ's signature frequencies. With this precoder the signal component $\mathbf{D}_\mu\mathbf{\Theta}_\mu\mathbf{s}_\mu(i)$ of $\tilde{\mathbf{x}}_\mu(i)$ in (20) is the product of the μth channel's DTFT with the DTFT of the symbols $\mathbf{s}_\mu(i)$ evaluated at user μ's signature frequencies. Hence, $\mathbf{D}_\mu\mathbf{\Theta}_\mu\mathbf{s}_\mu(i)$ is just the DTFT of the convolution between the channel $h_\mu(n)$ and the symbols in $\mathbf{s}_\mu(i)$. Let us define a $J \times J$ Vandermonde matrix $\bar{\mathbf{\Theta}}_\mu$ with $(p+1, q+1)$st entry $\rho_{\mu,p}^{-q}$. Similar to $\mathbf{\Theta}_\mu$, pre-multiplication of a $J \times 1$ vector by $\bar{\mathbf{\Theta}}_\mu$ evaluates its DTFT at the signature frequencies. Defining $\bar{\mathbf{x}}_\mu(i) := A_\mu^{-1}\bar{\mathbf{\Theta}}_\mu^{-1}\tilde{\mathbf{x}}(i)$, where $\bar{\mathbf{\Theta}}_\mu^{-1}$ performs the inverse DTFT, we get back the time-domain convolution as [22]:

$$\bar{\mathbf{x}}_\mu(i) = \bar{\mathbf{H}}_\mu\mathbf{s}_\mu(i) + A_\mu^{-1}\bar{\mathbf{\Theta}}_\mu^{-1}\mathbf{\Gamma}_\mu\mathbf{\Phi}_\mu^T\mathbf{F}\tilde{\boldsymbol{\eta}}(i) \tag{23}$$

$$:= \bar{\mathbf{H}}_\mu\mathbf{s}_\mu(i) + \bar{\boldsymbol{\eta}}_\mu(i) \tag{24}$$

where we have defined $\bar{\boldsymbol{\eta}}_\mu(i) := A_\mu^{-1}\bar{\mathbf{\Theta}}_\mu^{-1}\mathbf{\Gamma}_\mu\mathbf{\Phi}_\mu^T\mathbf{F}\tilde{\boldsymbol{\eta}}(i)$ and the single user channel matrix $\bar{\mathbf{H}}_\mu$ is $J \times K$ Toeplitz as in (7). Matrix $\bar{\mathbf{H}}_\mu$ is always full rank, which confirms that under design condition (21) our precoders guarantee symbol recovery. Therefore, pre-multiplication by $\bar{\mathbf{\Theta}}_\mu^{-1}$ converts our system to M parallel single user channels [21] (see also Figure 13). Such an equivalence is not only conceptually neat: it also implies that any single user equalizer designed for single user block transmissions is also applicable to the GMC-CDMA setup following the MUI elimination stage. For example, subspace and finite-alphabet based blind channel estimators for block transmissions with ZP are directly applicable and have been considered in [22], [69], [72].

We remark that if the channel is going to be estimated

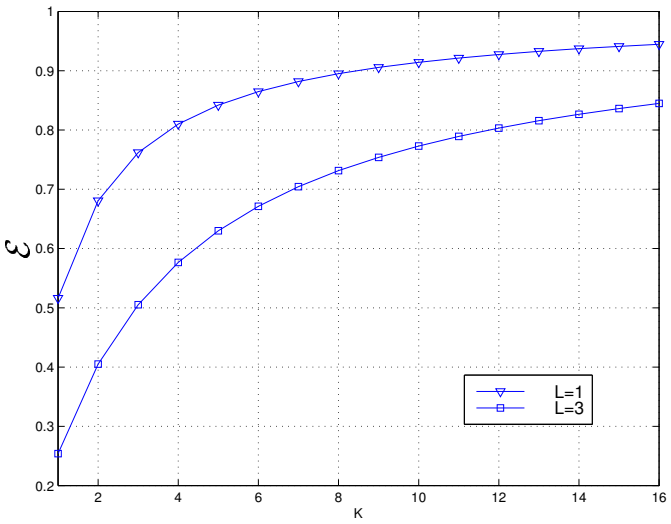

Fig. 14. Bandwidth efficiency for GMC-CDMA of 16 users

through training, we can select $J = K + \tilde{L} \leq K + L$ without loosing symbol detectability. But for blind channel estimation using the subspace techniques in [53], one still needs $J = K + L$.

D. Design Considerations

We have so far been able to design multiuser transceivers that are MUI/ISI-resilient and guarantee symbol recovery. In wireless applications however, there are additional design parameters that deserve further elaboration.

Choice of parameters:: How should one choose the block length K, the number of redundant symbols L, and the number of users M that can be accommodated? From a bandwidth utilization point of view, each of the M users sends K information symbols every $P = N+L = MJ+L$ transmitted symbols (that include the length-L CP, which is common to all the users and takes off IBI). Therefore, it is meaningful to define bandwidth efficiency as

$$\mathcal{E} := \frac{MK}{P} = \frac{MK}{M(K+L)+L} \leq 1. \tag{25}$$

For fixed M and L, larger K implies higher bandwidth efficiency. This becomes clear in Figure 14, where the bandwidth efficiency of a system consisting of $M = 16$ users is depicted for $L = 1$ and 3 with K varying from 1 to 16. But as K increases, the demodulation latency increases as well, because the receiver needs to wait for the entire P-long block before demodulating symbols in the block. Furthermore, as K increases the complexity of the system grows accordingly, although only slightly faster than linear. Indeed, only $K \log K$ ($J \log J$ to be precise) increase in complexity is required for the two N-point FFTs involved — one at the transmitter and the other at the receiver (recall also that $N = M(K + L)$).

The parameter L can be computed approximately as follows: for a given bandwidth W, we determine the chip waveform duration to be about $T_c = 1/W$. Suppose that the physical subchannels have maximum delay spread upper bounded by $\tau_{\text{max,s}}$ and that the maximum relative delay among the users is $\tau_{\text{max,d}}$. Then L can be computed as $L = \lceil (\tau_{\text{max,s}} + \tau_{\text{max,d}})/T_c \rceil = \lceil (\tau_{\text{max,s}} + \tau_{\text{max,d}})W \rceil$, where $\lceil \cdot \rceil$ denotes integer-ceiling. Although L is expressed in terms of chips and therefore defines inter chip interference lengths, we have not posed any upper limit on L; thus, channels with ISI spanning multiple symbols are also allowed.

From (25), we deduce that the bandwidth efficiency is approximately $K/(K + L)$ for large K or M. So, given the desired bandwidth efficiency $\mathcal{E}$, which is certainly a major resource in wireless communications, we can figure out how large K should be by solving $\mathcal{E} = K/(K + L)$ while accounting also for demodulation delays and system complexity.

Apart from complexity, the parameter K also affects system performance. For example, as the number of subcarriers $N = M(K + L)$ increases with K, the subcarrier spacing becomes smaller, which implies increased susceptibility to frequency synchronization errors and/or time-varying (Doppler) fading effects. This imposes an upper limit on the maximum number of users supportable once K is fixed, because the physical subcarrier spacing is $W/(MJ)$.

Subcarrier allocation:: In deriving our MUI-resilient GMC-CDMA system of (16) – (21), we have selected users' signature frequencies that are non-overlapping (c.f. (15)). Absence of a specific rule for distributing the N subcarriers in $\mathcal{F}$ to the M users offers flexibility to our design, because any allocation scheme obeying (15) will have built-in deterministic MUI elimination and will guarantee symbol recovery. In fact, extra degrees of freedom emerge if the subcarriers obeying (15) are allowed to have different amplitudes as well. This corresponds to replacing the FFT matrices $\mathbf{F}$, $\mathbf{F}^{\mathcal{H}}$ in (16) by Vandermonde matrices as detailed in [21], [22], [67]–[69]. Our choice to stick with constant modulus (CM) complex exponentials here is motivated by the low-complexity of FFT-based designs. But in general, all allocation schemes that satisfy (15) will not lead to the same BER. So there is a possibility for optimization and pertinent criteria could aim at maximizing information rate, minimizing BER, or minimizing symbol MSE. We do not have available algorithms for optimum allocation when CSI is available at the mobiles, but this is certainly a very interesting problem for future research.

Even without an optimum design, (possibly random) dynamic frequency allocation within the class of (15), might still be helpful. Such dynamic frequency allocation could consist of frequency hopping where the users rely on non-overlapping subcarriers to achieve frequency diversity gains. Spreading each user's subcarriers as far as possible is also well motivated when no CSI is available at the transmitters. A special yet important design is to allocate the N subcarriers to the M users in a cyclic fashion; e.g., we can set $\forall \mu \in [0, M-1]$

$$\rho_{\mu,l} = e^{j\frac{2\pi}{N}(lM+\mu)}, \quad l \in [0, J-1]. \tag{26}$$

It turns out that such a choice for the signature frequencies combined with the choice (22) for $\mathbf{\Theta}_\mu$, results in a very simple spreading code matrix that is expressible as (c.f. (16)):

$$\mathbf{C}_\mu = A_\mu \mathbf{f}_\mu \otimes [\mathbf{I}_K \ \mathbf{0}_{K\times L}]^T, \tag{27}$$

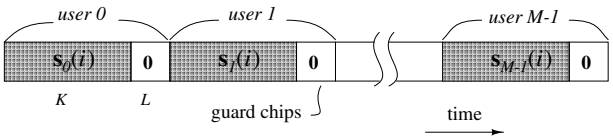

Fig. 15. ZP-only/TDMA block spreading scheme

where $\mathbf{f}_\mu := M^{-\frac{1}{2}}[1, \exp(j\frac{2\pi\mu}{M}), \ldots, \exp(j\frac{2\pi\mu}{M}(M-1))]^T$ is the $(\mu+1)$st column of an $M \times M$ IFFT matrix. The GMC-CDMA transmitter corresponding to (27) involves a two-layer spreading process: the inner layer, represented by the $[\mathbf{I}_K \ \ \mathbf{0}_{K\times L}]^T$ matrix, implements single user ZP-only transmissions with L trailing zeros; the outer layer represented by the IFFT column vector $\mathbf{f}_\mu$, corresponds to an FDMA scheme, where the transmitted symbols are the entries of the ZP-only-precoded inner layer block. While the outer layer code $\mathbf{f}_\mu$ takes care of MUI elimination, the inner layer code offers channel-independent (blind) symbol recovery thanks to the redundancy introduced. Prompted by this two-layer ZP-only/FDMA spreading approach, one may envision additional spreading code designs such as ZP-only/TDMA, FDM/TDMA, and FDM/FDMA. As an example, user μ's spreading code matrix in a ZP-only/TDMA paradigm will be given as $\mathbf{C}_\mu = A_\mu \mathbf{e}_\mu \otimes [\mathbf{I}_K \ \mathbf{0}_{K\times L}]^T$, where $\mathbf{e}_\mu$ is the $(\mu+1)$st column of an $M \times M$ identity matrix $\mathbf{I}_M$ (see Figure 15).

We can also verify that matrix $\mathbf{C}_\mu$ in (27) is a Toeplitz convolution matrix, which implies that this particular spreading amounts to a convolution. Indeed, block $\mathbf{u}(i)$ is the convolution of the first column in $\mathbf{C}_\mu$ with $\mathbf{s}_\mu(i)$. Interpreting spreading as convolution applies to all our code designs when $\mathbf{\Theta}_\mu$ is chosen as in (22), only the convolution is generally a circular one. It reduces to linear convolution in this case because the first column of $\mathbf{C}_\mu$ has more than K trailing zeros. Such a "convolutional spreading" includes symbol-periodic spreading (DS-SS) as a special case. It is also reminiscent of cyclic block channel codes over the Galois field. Links and jointly optimal designs of the spreading codes constructed here in the complex field and the channel error control codes typically designed in the Galois field is another interesting future topic.

Multicarrier yet constant modulus?: A closer inspection of the $\mathbf{C}_\mu$ structure in (27) will reveal presence of many zero entries. It turns out in fact, that the linear convolution implementing $\mathbf{C}_\mu$ at the transmitter involves only shifting and scaling (by modulus-one exponentials) [22]. In addition to being attractive from a complexity perspective, such a spreading retains (except for a "transmission gap" of length L) the CM property provided that symbols in $\mathbf{s}_\mu(i)$ are CM. This unique feature of GMC-CDMA relieves the HPA from high PAR problems, without sacrificing the benefits arising from MC modulation. Such codes are potentially useful even to single user OFDM system for PAR reduction.

Example 2: To further reveal the MC nature in our GMC spreading code design, Figure 16a depicts the DTFT of the first column (that will be convolved with the information symbols) of each user's spreading matrix $\mathbf{C}_\mu$ in (27). Parameter choices here are $M = 3$, $K = 4$, and $L = 1$. As we can see, corresponding to the subcarrier allocation (26), the users' spreading codes have interleaved sinc-like spectra. In Figure 16b, we depict the DTFT of a received block. With spreading codes as in (27), the three users transmit pseudo-random ± 1 symbols through channels with nulls at $-j$, -0.5, -0.7, respectively. As we can see, at the user 0's signature frequencies, only the signal from user 0 is non-zero (ignoring noise). Since $L = 1$, at most one of the $K + L = 5$ subcarriers can undergo fading by channel nulls; $K = 4$ information symbols are thus recoverable because at least $5 - 1 = 4$ subcarriers will survive. In Figure 16b, one of the signature frequencies is close to the channel null at $\exp(-j0.5\pi)$ and is considerably attenuated. In an OFDMA or other single-subcarrier-per-information-symbol systems, such a case would pose serious symbol recovery problems or at least severe performance degradation.

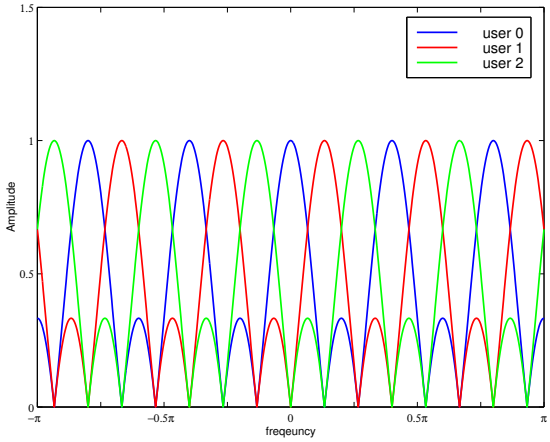

Fig. 16a. DTFT of GMC-CDMA codes

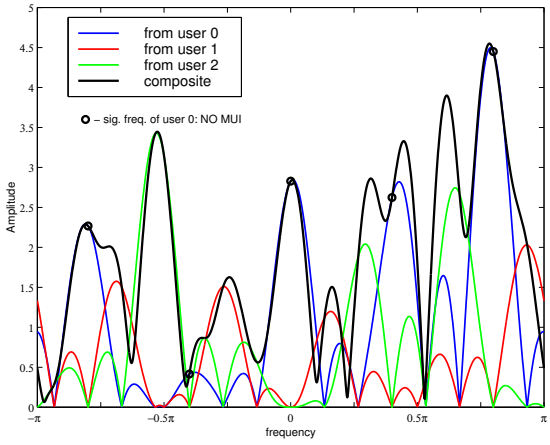

Fig. 16b. DTFT of the received block

Precoder and equalizer design:: Another factor in designing $\mathbf{C}_\mu$'s that deserves further discussion is our choice of the precoding matrices $\mathbf{\Theta}_\mu$, that are required to satisfy (21). We have concluded that for (21) to hold regardless of the underlying channels, any $J - L = K$ rows of $\mathbf{\Theta}_\mu$ should be linearly independent. When CSI is available at the transmitters, we can choose $J = K$ (instead of $J = K + L$) to avoid channel nulls and still be able to satisfy (21). The idea is similar to a multi-user DMT: allocate frequencies to each user that do not coincide with the user's channel nulls (since we

know them). On the other hand, it is also possible to choose $J > K+L$, in which case $\mathbf{\Theta}_\mu$'s can be designed such that any $J-L$ rows span the $\mathbb{C}^K$ space of complex K-tuples in order to guarantee (21). Choosing J large can be useful when the system is underloaded; i.e., when the number of active users is less than the maximum M that can be supported by the available bandwidth [18], [20]. In this case, each user can be allocated more than $K+L$ subcarriers and different SS codes $\mathbf{\Theta}_\mu$ can be assigned to gain in BER performance. Furthermore, we could increase K to accommodate users with higher rates. We will elaborate further on the multirate capabilities of GMC-CDMA shortly.

It is also possible to optimize the design of $\mathbf{\Theta}_\mu$ over the class of MUI-resilient models in (17). Given the allocated signature subcarriers of user μ and the μth channel (hence the diagonal matrix $\mathbf{D}_\mu$), we can optimize the performance by minimizing MSE, or, maximizing information rate by choosing judiciously matrices $\mathbf{\Theta}_\mu$ and $\mathbf{\Gamma}_\mu$ along the lines of [51].

Multirate designs for multimedia services:: Capability to offer different users different and/or variable transmission rates is a very attractive feature, especially for certain multimedia applications. It turns out that such services can be provided using our framework easily. The basic idea is to allow different users to have different number of subcarriers [68]. As long as we keep the number of subcarriers J_μ allocated to user μ greater than L, we can guarantee symbol recovery by transmitting $J_\mu - L$ symbols on those J_μ subcarriers through proper precoder design. Hence, given a total of N system subcarriers, the number of subcarriers allocated to users should satisfy the following constraints:

$$J_\mu > L,\ \forall \mu \in [0, M-1], \quad \text{and} \quad \sum_{\mu=0}^{M-1} J_\mu = N. \qquad (28)$$

Note that the sets of subcarriers allocated to different users can be non-intersecting as in (15) even when each $\mathcal{F}_\mu$ has different cardinality (different number of subcarriers J_μ per user). Indeed, reflecting on our single-rate GMC-CDMA design reveals that the orthogonality in (19) applies to the multirate case as well. With J_μ subcarriers, the μth user can transmit $K_\mu = J_\mu - L$ symbols with guaranteed recovery through channels that are blindly identifiable as in our single rate system.

The advantage of our multirate GMC-CDMA scheme, compared to existing multirate CDMA alternatives (multicode and variable spreading length CDMA, see e.g., [29], [36]), is that it offers easier rate switching capability, finer rate resolution and in general better average BER performance [68]. Perhaps more important, following the MUI elimination step, GMC-CDMA enables application of the single-rate single-user *blind* channel estimation and equalization algorithms even to the *multirate* case. Since user μ can transmit $K_\mu = J_\mu - L$ symbols with P chips, we define the μth user's *symbol rate* (measured in symbols per second) as $R_\mu := K_\mu/(PT_c)$. With this definition, we have established the following result for multirate GMC-CDMA [68].

Result 2: For channels of order L, as per Assumption 2, and users of prescribed rates $R_0, \ldots, R_{M-1}$ that satisfy $R_T = \sum_{\mu=0}^{M-1} R_\mu < 1/T_c$, it is possible to choose J_μ, $\forall \mu \in [0, M-1]$, such that $(J_\mu - L)/(PT_c) \geq R_\mu$ with $P = \sum_{\mu=0}^{M-1} J_\mu + L$. That is, under Assumption 2, MUI/ISI-free transmissions at or above the specified rates are possible regardless of multipath channels up to order L with guaranteed (even blind) channel identifiability and symbol recovery.

Example 3: To demonstrate the feasibility of blind equalization in the multirate setup, we simulated a multirate GMC-CDMA system with $N = 220$ subcarriers equally spaced on the unit circle (as in (26)). There are $M = 8$ users in the system (4 users with low rate R_L and 20 subcarriers each and 4 users with double rate $R_H = 2R_L$ and 35 subcarriers each). Each channel is assumed to have $L = 5$ taps simulated as complex Gaussian random deviates of equal variance. One hundred channel realizations were simulated for each user and 100 received blocks were processed by the receiver to estimate the users' channels. MMSE equalization was employed after blind channel estimation and compared with MMSE equalization results obtained with known CSI. Figure 17 shows that blind MMSE equalizers for multirate GMC-CDMA perform on the average only 2–4 dB below the ideal MMSE equalizer.

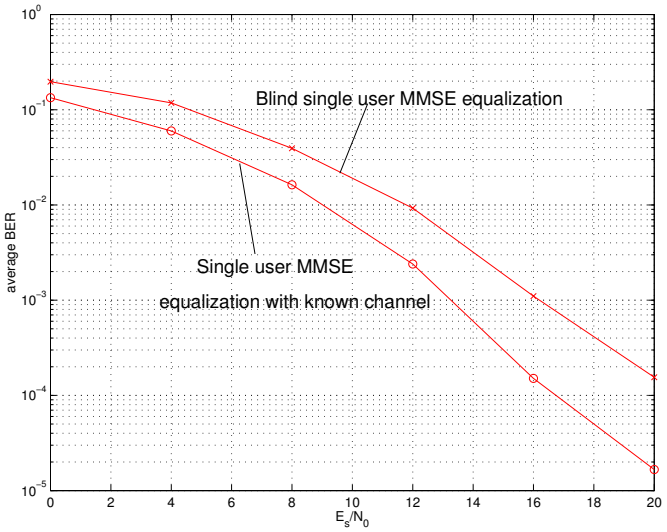

Fig. 17. Blind equalization for multirate GMC-CDMA

Real code designs for baseband services:: We have designed spreading codes over the complex field up to now. For most systems, the complex transmission will be modulated on the in-phase and quadrature-phase components if radio frequency (RF) carrier modulation[3] is involved. In baseband systems however, all signals involved are real. The MC (or multi-subcarrier) concept is still applicable, but we will need to induce symmetry on the subcarrier allocation so that the resulting codes can be real. To show how, let us define a mirror-augmentation operation on an $N \times K$ matrix $\mathbf{B}$ as the one that produces a $(2N-1) \times K$ matrix $\Xi\{\mathbf{B}\}$, which holds $\mathbf{B}$ on its first N rows and the row-wise flipped and conjugated version of $\mathbf{B}$ in the remaining $N-1$ rows. Specifically, the

[3]Unlike our discrete-time subcarriers discussed throughout the paper, carrier here refers to the continuous time $\exp(j2\pi f_c t)$ with RF f_c in Hz.

$(2N-p)$th row of $\Xi\{\mathbf{B}\}$ is the conjugate of the $(p+1)$st row of $\mathbf{B}$. So constructed, matrix $\Xi\{\mathbf{B}\}$ possesses row-wise conjugate symmetry in the sense that any two rows are conjugates of each other if the their row indices sum up to $2N+1$. Relying on this mirror mapping, we can replace our $N \times K$ code design in (16) by the $(2N-1) \times K$ precoder matrix

$$\bar{\mathbf{C}}_\mu = \mathbf{F}^{\mathcal{H}}_{2N-1} \Xi\{\mathbf{\Phi}_\mu \mathbf{\Theta}_\mu\}, \tag{29}$$

where $\mathbf{F}^{\mathcal{H}}_{2N-1}$ is a $(2N-1)$-point IFFT matrix. Code matrix $\bar{\mathbf{C}}_\mu$ is real thanks to the conjugate symmetry we built through $\Xi\{\cdot\}$. Aiming at real codes that require symmetric code designs, we drop the transmission rate by almost 50% since we have to use almost twice as many subcarriers. Construction of real codes is important though in baseband applications such as impulse radio, which has been shown recently to fall also under the umbrella of the GMC-CDMA block spreading model [33]. Real GMC-CDMA spreading codes can also be potentially useful for baseband wireline multiuser DSL transmissions.

E. Comparisons with MC-CDMA

As we mentioned in Section IV-B, our GMC-CDMA block spreading model subsumes many MC schemes, including MC-CDMA, as a special case [19], [20], [67]. In this subsection, we show how MC-CDMA can be described using our GMC-CDMA system setup and then compare its BER performance with that of our MUI-free GMC-CDMA design.

MC-CDMA is also called OFDM-CDMA, because each user spreads one symbol ($K=1$) using a unique spreading sequence and then performs an OFDM modulation so that each chip in the spreading sequence modulates one of the N subcarriers. The subcarriers are shared by all the users and user separation is accomplished thanks to the linear independence among user-specific spreading sequences. To implement MC-CDMA one simply needs to specialize our GMC-CDMA code design (16) as follows: i) $\mathbf{\Phi}_\mu \to \mathbf{I}_N$; ii) matrix $\mathbf{\Theta}_\mu \to \mathbf{c}_\mu$, where $\mathbf{c}_\mu$ is an $N \times 1$ vector specifying user μ's spreading code. That is, MC-CDMA uses (16) with $\mathbf{C}_\mu \to \mathbf{F}^{\mathcal{H}} \mathbf{c}_\mu$. Since DS-CDMA amounts to replacing $\mathbf{C}_\mu$ by $\mathbf{c}_\mu$, the difference between MC-CDMA and DS-CDMA comes mainly from the OFDM modulation performed via the IFFT matrix $\mathbf{F}^{\mathcal{H}}$. As in multicode DS-CDMA, multiple spreading codes can also be allocated to each MC-CDMA user to enable simultaneous transmissions of multiple symbols. The difference between MC-CDMA and our MUI/ISI-resilient GMC-CDMA design lies in two points:

i) GMC-CDMA assigns distinct subcarriers to different users as per (15);

ii) GMC-CDMA blocks K (>1) transmitted symbols and judiciously adds redundancy through the $(K+L) \times K$ linear precoder $\mathbf{\Theta}_\mu$ that renders each user's transmission robust against frequency selective fading (c.f. (21)).

Example 4: To illustrate the advantage of our MUI-free GMC-CDMA system design over alternatives that do not assure MUI-elimination such as MC-CDMA, we compare their performance in multipath fading channels of order $L=2$ with equal variance complex Gaussian taps. GMC-CDMA has parameters $(L,K,M)=(2,8,14)$ and adopts the frequency allocation scheme in (26) and the precoder of (22). For the MC-CDMA system, each user spreads 14 symbols each with a different Walsh-Hadamard sequence of length $N=M(K+L)=128$ and then modulates the sum using OFDM with CP of length $L=2$. Receivers of both systems assume perfect CSI and they both use MMSE equalization. As can be seen from Figure 18, the MUI-free GMC-CDMA system outperforms MC-CDMA by about 5dB at BER $\approx 10^{-3}$.

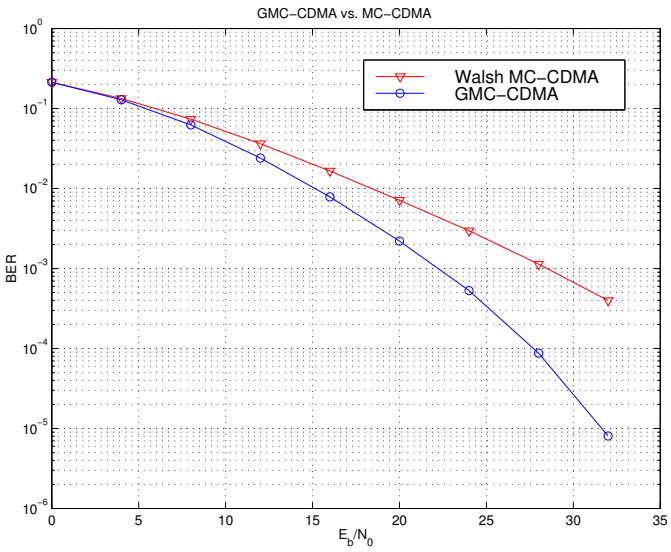

Fig. 18. GMC-CDMA vs. Walsh-spread MC-CDMA

V. Conclusions and Discussion

We have demonstrated the importance of transmitting in blocks at both the information symbol level and at the chip sequence level. We also highlighted the attractive FFT features inherent to wireless MC transmissions. We have shown that both cyclic-prefixing (CP) and zero-padding (ZP) can achieve IBI-free reception. While CP enables simple equalization of multipath channels, ZP offers guaranteed symbol recovery regardless of where channel fades may appear. In addition, a ZP transmission can be recast as a CP transmission by appropriately overlapping and adding successive blocks at the receiver. Therefore, ZP appears to be more flexible than CP: it can trade-off equalization complexity with symbol detectability (which has a major impact on performance as we illustrated in Figure 12). We also pointed out the potential of CP-only and ZP-only block transmissions that do not introduce high peak-to-average power ratio while incurring only a slight increase in receiver complexity.

Comparing serial- with block- equalization, we concluded that block receivers (especially the ZP option) are capable of equalizing non-minimum phase channels with causal and stable FIR block equalizers, without restrictions on channel null locations. We discussed three block equalization schemes: pre-, post-, and balanced-equalization and highlighted their relative merits. When no CSI is available at the transmitter, IFFT precoding at the transmitter and FFT at the receiver

leads to OFDM which is an attractive single-user MC modulation scheme that affords simple FFT-based low complexity equalization. Symbol recovery in CP-OFDM suffers when the channel has zeros on the FFT grid. To correct worst case (channel-induced) symbol errors using linear block error-correcting codes, one should be willing to pay a two-fold increase in redundancy relative to that needed for the uncoded CP-OFDM. This motivated in part our GMC-CDMA multicarrier transmission that offers guaranteed symbol recovery with minimum transmit-redundancy (and thus maximum bandwidth efficiency).

Relying on information symbol blocking and an FDMA-like approach implemented via FFTs, we were able to design an MUI-free block spreading generalized multicarrier CDMA system that guarantees (even blind) symbol recovery regardless of the multipath channels involved. We showed that it also renders the multiple access channels equivalent to independent parallel single-user channels, where per-user equalization and transmitter-receiver optimization can be carried out using existing single-user techniques. Especially in the uplink, GMC-CDMA outperforms other multiple access schemes including MC-CDMA. It also enables blind channel identification of all users' channels regardless of channel null locations. Simulations illustrated that blind schemes have quite acceptable performance relative to theoretical performance with known CSI.

In GMC-CDMA, multirate services can be incorporated while preserving MUI-resilience by allocating different number of subcarriers to different rate users. We also showed that specific choices of the subcarrier allocation and precoder designs yield MC transmissions with (almost) constant modulus, which is quite advantageous since existing MC schemes are known to suffer from high peak-to-average power ratio problems. Additional low complexity constant modulus GMC-CDMA systems, such as ZP-only/TDMA, FDM-TDMA, FDM-FDMA, schemes were briefly mentioned and they will be explored elsewhere.

MUI/ISI-resilience with bandwidth and power efficiency in the uplink are unique features of our GMC-CDMA spreading code design and pay off in additional applications. For example, GMC-CDMA has been successfully applied to space-time coding [35] and the problem of designing jointly the network, data-link, and physical layers for integrated system performance optimization [56].

Our block spreading approach to multiuser communications is in the same spirit of (and can be nicely motivated by) Shannon's introduction of block-code length as the third powerful resource for designing reliable systems without intervention of the other two major resources, namely power and bandwidth. To appreciate the link with our MUI- and ISI-limited multiuser context, we can ask ourselves this question: How do existing multiple access schemes utilize the available resources to combat MUI and channel-induced fading? Before answering, let us recall that transmissions "hit by a channel null (fade)" are a measure-zero event but being in a "fading neighborhood" may be very likely especially when many users transmit through channels with long delay spreads. Capitalizing on the first resource, *power control* clearly offers an answer because by increasing the power one can overcome even deep channel fades and severe MUI. However, power control entails considerable overhead and in principle it goes against the basic premise of CDMA that requires minimal co-ordination among users through the BS. On the other hand, direct-sequence (DS), frequency-hopping (FH), and existing multi-carrier CDMA hybrids rely on the second resource to mitigate MUI and ISI by expanding the *bandwidth* beyond the minimum required for a given number of users. When bandwidth is at a premium and power-limited mobiles transmit in the uplink, neither of these answers seems more appealing relative to our approach. GMC-CDMA relies on symbol blocking and thus exploits the third resource (length of *block spreading* codes) at the expense of longer delays in demultiplexing. Interestingly though, our complexity can be almost linear (FFT based) which is in sharp contrast with approaches that have advocated error control codes for MUI/ISI elimination in multiuser systems and necessitate complex decoding in addition to long delays and bandwidth over-expansion [31], [66], [46], [47].

Acknowledgments:: This research was supported by NSF CCR Grant No. 98-05350; the NSF Wireless Initiative Grant No. 99-79443; the ARO Grant No. DAAG55-98-1-0336, and the ARL Grant No. DAAL01-98-Q-0648.

REFERENCES

[1] I. 802.11, "IEEE standard for wireless LAN medium access control (MAC) and physical layer (PHY) specifications," Nov. 1997.

[2] J. A. C. Bingham, "Multicarrier modulation for data transmission: An idea whose time has come," *IEEE Communications Magazine*, pp. 5–14, May 1990.

[3] J. A. C. Bingham, *ADSL, VDSL, and Multicarrier Modulation*, Wiley-Interscience, 2000.

[4] J. S. Chow, J. C. Tu, and J. M. Cioffi, "A discrete multitone transceiver system for HDSL applications," *IEEE Journal on Selected Areas in Communications*, vol. 9, no. 6, pp. 895–908, Aug. 1991.

[5] P. S. Chow, J. M. Cioffi, and J. A. C. Bingham, "A practical discrete multitone transceiver loading algorithm for data transmission over spectrally shaped channels," *IEEE Trans. Commun.*, vol. 73, no. 2, pp. 773–775, Feb./Mar./Apr. 1995.

[6] P. S. Chow, J. C. Tu, and J. M. Cioffi, "Performance evaluation of a mutlichannel transceiver system for ADSL and VHDSL services," *IEEE Journal on Selected Areas in Communications*, vol. SAC-9, no. 6, pp. 909–919, Aug. 1991.

[7] L. J. Cimini Jr., "Analysis and simulation of a digital mobile channel using orthogonal frequency division multiplexing," *IEEE Trans. Commun.*, vol. COM-33, no. 7, pp. 665–675, July 1985.

[8] B. P. Crow, I. Widjada, J. G. Kim, and P. T. Sakai, "IEEE 802.11 Wireless Local Area Networks," *IEEE Communications Magazine*, pp. 116–126, Sept. 1997.

[9] D. Dardari and V. Tralli, "High-speed indoor wireless communications at 60 GHz with coded OFDM," *IEEE Trans. Commun.*, vol. 47, no. 11, pp. 1709–1721, Nov. 1999.

[10] V. M. DaSilva and E. S. Sousa, "Multicarrier orthogonal CDMA signals for quasi-synchronous communication systems," *IEEE Journal on Selected Areas in Communications*, pp. 842–852, June 1994.

[11] ETSI, "Radio equipment and systems, HIgh PErformance Radio Local Area Network (HIPERLAN) Type 1," *European Telecommunication Standard, ETS*, 300–652, Oct. 1996.

[12] ETSI, "Digital video broadcasting: Framing structure, channel coding, and modulation for digital terrestrial television," *European Telecommunication Standard*, EN 300–744, Aug. 1997.

[13] ETSI, "Radio broadcasting systems; Digital Audio Broadcasting (DAB) to mobile, portable and fixed receivers," *ETS 300 401 ed.2*, May 1997.

[14] ETSI, "Broadband Radio Access Networks (BRAN); HIPERLAN Type 2 technical specification Part 1 — physical layer," *DTS/BRAN030003-1*, Oct. 1999.

[15] K. Fazel and G. P. F. (Eds), *Multi-Carrier Spread Spectrum*, Kluwer Academic Publishers, 1997.

[16] D. Gesbert, J. Sorelius, and A. Paulraj, "Blind multi-user MMSE detection of CDMA signals," in *Proc. of IEEE Intl. Conf. on Acoustics, Speech, and Signal Processing*, pp. 3161–3164, May 1998.

[17] G. B. Giannakis, "Filterbanks for blind channel identification and equalization," *IEEE Signal Processing Lett.*, vol. 4, pp. 184–187, June 1997.

[18] G. B. Giannakis, P. A. Anghel, and Z. Wang, "Wideband generalized multi-carrier CDMA over frequency-selective wireless channels," in *Proc. of IEEE Intl. Conf. on Acoustics, Speech, and Signal Processing*, Istanbul, Turkey, pp. 2501–2504, June 5–9, 2000.

[19] G. B. Giannakis, P. A. Anghel, and Z. Wang, "Generalized multi-carrier CDMA: Unification and linear equalization," *EURASIP Journal on Applied Signal Processing*, pp. 743–756, Apr. 2005.

[20] G. B. Giannakis, A. Stamoulis, Z. Wang, and P. Anghel, "Load-adaptive MUI/ISI-resilient generalized multi-carrier CDMA with linear and decision-feedback equalizers," *European Trans. on Telecomm.*, vol. 11, no. 6, pp. 527–537, Nov./Dec 2000.

[21] G. B. Giannakis, Z. Wang, A. Scaglione, and S. Barbarossa, "Mutually orthogonal transceivers for blind uplink CDMA irrespective of multipath channel nulls," in *Proc. of IEEE Intl. Conf. on Acoustics, Speech, and Signal Processing*, Phoenix, AZ, vol. 5, pp. 2741–2744, Mar. 1999.

[22] G. B. Giannakis, Z. Wang, A. Scaglione, and S. Barbarossa, "AMOUR — Generalized Multicarrier Transceivers for Blind CDMA regardless of Multipath," *IEEE Trans. Commun.*, vol. 48, no. 12, pp. 2064–2076, Dec. 2000.

[23] K. S. Gilhousen, I. M. Jacobs, R. Padovani, A. J. Viterbi, L. A. Weaver, and C. E. W. III, "On the capacity of a cellular CDMA system," *IEEE Trans. on Vehicular Tech.*, vol. 40, no. 2, pp. 303–312, May 1991.

[24] G. H. Golub and C. F. van Loan, *Matrix Computations*, Johns Hopkins Univ. Press, 3rd edition, 1996.

[25] S. Hara and R. Prasad, "Overview of multicarrier CDMA," *IEEE Communications Magazine*, pp. 126–133, Dec. 1997.

[26] H. Harashima and H. Miyakawa, "Matched-transmission technique for channels with intersymbol interference," *IEEE Trans. Commun.*, vol. COM-20, no. 4, pp. 774–780, Aug. 1972.

[27] R. W. Heath Jr. and G. B. Giannakis, "Exploiting input cyclostationarity for blind channel identification in OFDM systems," *IEEE Trans. Signal Processing*, vol. 47, no. 3, pp. 848–856, Mar. 1999.

[28] D. Hughes-Hartogs, "Ensemble modem structure for imperfect transmission media," *U.S. Patent No. 4833706*, May 1989.

[29] A.-L. Johansson and A. Svensson, "On multirate DS-CDMA schemes with interference cancellation," *Journal on Wireless Personal Communications*, vol. 9, no. 1, pp. 1–29, Jan. 1999.

[30] D. C. Jones, "Frequency domain echo cancellation for discrete multitone asymmetric digital subscriber line transceivers," *IEEE Trans. Commun.*, vol. 43, no. 2/3/4, pp. 1663–1672, Feb./Mar./Apr. 1995.

[31] S. Kaiser and K. Fazel, "A spread spectrum multi-carrier multiple access system for mobile communications," in *MCSS*, Oberpfaffenhofen, Germany, pp. 49–56, Kluwer Academic Publishers [15], 1997.

[32] S. Kondo and L. B. Milstein, "Performance of multicarrier DS CDMA systems," *IEEE Trans. Commun.*, vol. 44, no. 2, pp. 238–46, Feb. 1996.

[33] C. Le Martret and G. B. Giannakis, "All-digital PPM impulse radio for multiple access through frequency-selective multipath," in *Proc. of the 1st Sensor Array and Multichannel SP Workshop*, Boston, MA, Mar. 15-17, 2000.

[34] H. Liu and G. Xu, "A subspace method for signature waveform estimation in synchronous CDMA systems," *IEEE Trans. Commun.*, vol. 44, no. 10, pp. 1346–1354, Oct. 1996.

[35] Z. Liu and G. B. Giannakis, "Space-time coding with transmit antennas for multiple access regardless of frequency-selective multipath," in *Proc. of the 1st Sensor Array and Multichannel SP Workshop*, Boston, MA, Mar. 15-17, 2000.

[36] U. Mitra, "Comparison of Maximum-Likelihood-based detection for two multirate access schemes for CDMA signals," *IEEE Trans. Commun.*, vol. 47, no. 1, pp. 64–77, Jan. 1999.

[37] B. Muquet, M. de Courville, P. Duhamel, and V. Buzenac, "A subspace based blind and semi-blind channel identification method for OFDM systems," in *Proc. of IEEE Workshop on Signal Proc. Advances in Wireless Comm.*, Annapolis, MD, pp. 243–246, May 1999.

[38] B. Muquet, M. de Courville, G. B. Giannakis, Z. Wang, and P. Duhamel, "Reduced complexity equalizers for zero-padded OFDM transmissions," in *Proc. of IEEE Intl. Conf. on Acoustics, Speech, and Signal Processing*, Istanbul, Turkey, pp. 2973–2976, June 5–9, 2000.

[39] R. V. Nee and R. Prasad, *OFDM for Wireless Multimedia Communications*, Artech House Publishers, Jan. 2000.

[40] R. Nogueroles, M. Bossert, A. Donder, and V. Zyablov, "Improved performance of a random OFDMA mobile communication system," in *Proc. of IEEE Vehicular Technology Conf.*, Ottawa, Canada, vol. 3, pp. 2502–2506, May 1998.

[41] T. Ojanpera, "Overview of multiuser detection/interference cancellation for DS-CDMA," in *IEEE International Conference on Personal Wireless Communications*, New York, NY, pp. 115–119, 1997.

[42] T. Ojanpera and R. Prasad, "An overview of air interface multiple access for IMT-2000/UMTS," *IEEE Communications Magazine*, vol. 36, no. 9, pp. 82–86, 91–5, Sept. 1998.

[43] A. V. Oppenheim and R. W. Schafer, *Discrete-Time Signal Processing*, Prentice-Hall, Inc., 1989.

[44] G. C. Porter, "Error distribution and diversity performance of a frequency differential PSK HF modem," *IEEE Trans. Commun.*, vol. COM-16, pp. 567–575, Aug. 1968.

[45] J. C. Rault, D. Castelain, and B. L. Floch, "The coded orthogonal frequency division multiplexing (COFDM) technique, and its application to digital radio broadcasting towards mobile receivers," in *Proc. of IEEE GLOBECOM*, Dallas, Texas, pp. 428–432, Nov. 1989.

[46] D. N. Rowitch and L. B. Milstein, "Convolutionally coded multicarrier DS-CDMA systems in a multipath fading channel — Part I: Performance analysis," *IEEE Trans. Commun.*, vol. 47, no. 10, pp. 1570–1582, Oct. 1999.

[47] D. N. Rowitch and L. B. Milstein, "Convolutionally coded multicarrier DS-CDMA systems in a multipath fading channel — Part II: Narrowband interference suppression," *IEEE Trans. Commun.*, vol. 47, no. 11, pp. 1729–1736, Nov. 1999.

[48] M. Russel and G. L. Stüber, "Terrestrial digital video broadcasting for mobile reception using OFDM," *Wireless Personal Communications*, vol. 2, no. 1–2, pp. 45–66, 1995.

[49] H. Sari, "Orthogonal frequency-division multiple access with frequency hopping and diversity," in *MCSS*. pp. 57–68, Kluwer Academic Publishers [15], 1997.

[50] H. Sari and G. Karam, "Orthogonal frequency-division multiple access and its application to CATV network," *European Trans. on Telecomm.*, vol. 9, no. 6, pp. 507–516, Nov.–Dec. 1998.

[51] A. Scaglione, S. Barbarossa, and G. B. Giannakis, "Filterbank transceivers optimizing information rate in block transmissions over dispersive channels," *IEEE Trans. Info. Theory*, vol. 5, no. 3, pp. 1019–1032, Apr. 1999.

[52] A. Scaglione, G. B. Giannakis, and S. Barbarossa, "Redundant filterbank precoders and equalizers Part I: Unification and optimal designs," *IEEE Trans. Signal Processing*, vol. 47, pp. 1988–2006, July 1999.

[53] A. Scaglione, G. B. Giannakis, and S. Barbarossa, "Redundant filterbank precoders and equalizers Part II: Blind channel estimation, synchronization, and direct equalization," *IEEE Trans. Signal Processing*, vol. 47, pp. 2007–2022, July 1999.

[54] A. Scaglione, G. B. Giannakis, and S. Barbarossa, "Linear precoding for estimation and equalization of frequency-selective channels," in *Signal Processing Advances in Wireless and Mobile Communications*, G. B. Giannakis, Y. Hua, P. Stoica, and L. Tong, Eds. vol. I, Chapter 9, Prentice-Hall, Inc, 2001.

[55] R. C. Singleton, "Maximum distance q-nary codes," *IEEE Trans. Info. Theory*, vol. 10, pp. 116–118, 1960.

[56] A. Stamoulis and G. B. Giannakis, "Packet fair queueing scheduling based on multirate multipath-transparent CDMA for wireless networks," *IEEE Trans. Commun.*, Aug. 1999 (submitted); see also *Proc. of INFOCOM*, Tel-Aviv, Israel, Mar. 26–30, 2000.

[57] A. Stamoulis, G. B. Giannakis, and A. Scaglione, "Block FIR decision-feedback equalizers for filterbank precoded transmissions with blind channel estimation capabilities," *IEEE Trans. Commun.*, vol. 49, pp. 69–83, Jan. 2001.

[58] V. Tarokh and H. Jafarkhani, "An algorithm for reducing the peak to average power ratio in a multicarrier communications system," in *Proc. of IEEE Vehicular Technology Conf.*, vol. 1, pp. 680–684, 1999.

[59] L. Thibault and M. T. Le, "Performance evaluation of COFDM for digital audio broadcasting part I: parametric study," *IEEE Trans. on Broadcasting*, vol. 43, no. 1, pp. 64–75, Mar. 1997.

[60] M. Tomlinson, "New automatic equaliser employing modulo arithmetics," *Electronics Letters*, vol. 7, no. 5–6, pp. 138–139, 1971.

[61] M. K. Tsatsanis and G. B. Giannakis, "Multirate filter banks for code-division multiple access systems," in *Proc. of IEEE Intl. Conf. on Acoustics, Speech, and Signal Processing*, New York, NY, USA, vol. 2, pp. 1484–1487, 1995.

[62] R. van Nee, G. Awater, M. Morikura, H. Takanashi, M. Webster, and K. W. Halford, "New high-rate wireless LAN standards," *IEEE Communications Magazine*, pp. 82–88, Dec. 1999.

[63] L. Vandendorpe, "Multitone spread spectrum multiple access communications system in a multipath Rician fading channel," *IEEE Trans. on Vehicular Tech.*, vol. 44, no. 2, pp. 327–337, May 1995.
[64] S. Verdú, *Multiuser Detection*, Cambridge Press, 1998.
[65] B. R. Vojčić and W. M. Jang, "Transmitter precoding in synchronous multiuser communications," *IEEE Trans. Commun.*, vol. 46, no. 10, pp. 1346–1355, Oct. 1998.
[66] X. Wang and H. V. Poor, "Iterative (Turbo) soft interference cancellation and decoding for coded CDMA," *IEEE Trans. Commun.*, vol. 46, no. 7, pp. 1046–1061, July 1999.
[67] Z. Wang and G. B. Giannakis, *Block Spreading for Multipath-Resilient Generalized Multi-Carrier CDMA*, vol. II, chapter 6, Prentice-Hall, Inc, Oct. 2000.
[68] Z. Wang and G. B. Giannakis, "Block Precoding for MUI/ISI-Resilient Generalized Multi-carrier CDMA with Multirate Capabilities," *IEEE Trans. Commun.*, vol. 49, no. 11, pp. 2016–2027, Nov. 2001.
[69] Z. Wang, A. Scaglione, G. B. Giannakis, and S. Barbarossa, "Vandermonde-Lagrange Mutually Orthogonal Flexible Transceivers for Blind CDMA in Unknown Multipath," in *Proc. of IEEE Workshop on Signal Proc. Advances in Wireless Comm.*, Annapolis, MD, pp. 42–45, May 9–12 1999.
[70] M. Zekri, P. Boets, and L. van Biesen, "DMT signals with low peak-to-average power ratio," in *Proc. IEEE International Symposium on Computers and Communications*, pp. 362–368, 1999.
[71] S. Zhou, G. B. Giannakis, and A. Scaglione, "Long codes for generalized FH-OFDMA through unknown multipath channels," *IEEE Trans. Commun.*, vol. 49, Apr. 2001.
[72] S. Zhou and G. B. Giannakis, "Finite-alphabet based channel estimation for OFDM and related multicarrier systems," *IEEE Trans. Commun.*, submitted Mar. 2000; see also *Conf. on Info. Sciences and Systems*, Princeton, NJ, March 15–17, 2000.
[73] M. S. Zimmerman and A. L. Kirsch, "The AN/GSC-10 (KATHRYN) variable rate data modem for HF radio," *IEEE Trans. Commun.*, vol. COM-15, pp. 197–205, Apr. 1967.
[74] W. Zou and Y. Wu, "COFDM: An overview," *IEEE Trans. on Broadcasting*, vol. 41, no. 1, pp. 1–8, Mar. 1995.

Z. Wang (Student Member) was born in Dalian, China, in 1973. He received his B.S. degree in Electrical Engineering and Information Science from the University of Science and Technology of China (USTC), Hefei, China, in 1996, and the the M.Sc. degree in Electrical Engineering from the University of Virginia, Charlottesville, in Dec. 1998.

He is now working towards the Ph.D. degree in the Department of Electrical and Computer Engineering, at the University of Minnesota. His broad interests lie in the areas of statistical signal processing and communications, including cyclostationarity, blind equalization algorithms, transceiver optimization, multicarrier, wideband multiple rate systems, and coding. His current interests focus on design and optimization of wireless multiuser communication systems.

G. B. Giannakis (Fellow) received his Diploma in Electrical Engineering from the National Technical University of Athens, Greece, 1981. From September 1982 to July 1986 he was with the University of Southern California (USC), where he received his MSc. in Electrical Engineering, 1983, MSc. in Mathematics, 1986, and Ph.D. in Electrical Engineering, 1986.

After lecturing for one year at USC, he joined the University of Virginia (UVA) in 1987, where he became a professor of Electrical Engineering in 1997, Graduate Committee Chair, and Director of the Communications, Controls, and Signal Processing Laboratory in 1998. He was awarded the School of Engineering and Applied Science Junior Faculty Research Award (UVA) in 1988, and the UVA-EE Outstanding Faculty Teaching Award in 1992. Since January 1999 he has been with the University of Minnesota as a professor of Electrical and Computer Engineering.

His general interests lie in the areas of signal processing and communications, estimation and detection theory, time-series analysis, and system identification – subjects on which he has published more than 100 journal papers. Specific areas of expertise have included (poly)spectral analysis, wavelets, cyclostationary, and non-Gaussian signal processing with applications to sensor array and image processing. Current research focuses on transmitter and receiver diversity techniques for equalization of single- and multi-user communication channels, mitigation of rapidly fading wireless channels, compensation of nonlinear amplifier effects, redundant filterbank transceivers for block transmissions, multicarrier, and wideband communication systems.

G. B. Giannakis received the IEEE Signal Processing Society's 1992 Paper Award in the Statistical Signal and Array Processing (SSAP) area, and co-authored the 1999 Best Paper Award by Young Author (M. K. Tsatsanis). He co-organized the 1993 IEEE Signal Processing Workshop on Higher-Order Statistics, the 1996 IEEE Workshop on Statistical Signal and Array Processing, and the first IEEE Signal Processing Workshop on Wireless Communications in 1997. He guest (co-)edited two special issues on high-order statistics (*International Journal of Adaptive Control and Signal Processing*, and the EURASIP journal *Signal Processing*), and the January 1997 special issue on signal processing for advanced communications (*IEEE Transactions on Signal Processing*). He has served as an Associate Editor for the *IEEE Transactions on Signal Processing* and the *IEEE Signal Processing Letters*, a secretary of the Signal Processing Conference Board, a member of the SP Publications board and a member and vice-chair of the SSAP Technical Committee. He now chairs the Signal Processing for Communications Technical Committee and serves as the Editor in Chief for the IEEE Signal Processing Letters. He is a member of the IEEE Fellow Election Committee and also a member of the European Association for Signal Processing.